Reaction Rate Predictions Via Group Additivity. Part 3: Effect of Substituents with CH_2 as the Mediator

Raman Sumathi,[†] Hans-Heinrich Carstensen,[‡] and William H. Green, Jr.*[,†]

Department of Chemical Engineering, Massachusetts Institute of Technology, 25 Ames Street, Cambridge, Massachusetts 02139

Received: October 25, 2001; In Final Form: March 19, 2002

In the first two papers of this series (Sumathi, R.; Carstensen, H.-H.; Green, W. H., Jr. *J. Phys. Chem.* **2001**, *105,* 6910. Sumathi, R.; Carstensen, H.-H.; Green, W. H., Jr. *J. Phys. Chem.* **2001**, *105,* 8969), a procedure has been developed on the basis of ab initio quantum chemical calculations to express the generic reaction rate in terms of the thermochemical contributions of the reactive moiety ("supergroup") in the transition structure. The supergroups are derived with the assumption that the contribution from the unreactive moiety to the thermochemistry is given by its group additivity (GA) values. This paper presents the qualitative justification for partitioning the energy of the transition structure into contributions from unreactive and reactive moieties using atoms in molecule (AIM) analysis. The couplings between these moieties, if any, are studied quantitatively using quantum chemical calculations at the CBS-Q level on reactions of the type $XCH_2CH_3 + Y \rightarrow XCH_2CH_2\bullet + HY$ (X = H, CH_3, $(CH_3)_2CH$, $(CH_3)_3C$, F, Cl, NH_2, SH, OH, OCH_3, OC(O)H, OC(O)-CH_3, CHO, $COCH_3$, COOH, $COOCH_3$, $CH{=}CH_2$, CCH; Y = H, CH_3). The present work thus focuses on the strength and limitations of the GA procedure and explores the effects of varying electronegative and bulky non-next-neighbor substituents, which are separated from the reactive center by a CH_2 group, on supergroup values. Both the C−H bond dissociation energies (BDE) and barrier heights to these reactions vary appreciably depending on the non-next-neighbor substituent, X. The preferred conformation around the XCH_2- - -CH_2(HY) bond in transition structures is largely determined by the effective hyperconjugative interaction between the bonds of the CH_2X group and the forming radical center. The effect of X on reaction barriers is subsequently modeled through a multilinear expression that is based on its inductive, steric, and hyperconjugative parameters, suggesting a practical way to accommodate non-next-neighbor effects on generic rate rules predicted using group additivity.

Introduction

In recent years, with the advance of high performance computers and user-friendly modeling and quantum chemistry software, significant efforts have been made to understand and model complex chemical reaction systems of industrial, environmental and atmospheric importance. Kinetic modeling of these chemical processes requires knowledge of literally thousands of rate constants at both very high (≳2000 K in combustion processes) and very low (∼200 K in upper atmospheric chemistry) temperatures over a broad range of pressures. The modelers use the experimental reaction rates whenever possible. Although some of the needed rate constants have been measured in the appropriate temperature and pressure regimes, there is still a large set of reactions that have been studied either only at usual laboratory temperatures or that, as yet, have no experimental data. The huge quantity of needed kinetic data for modeling (i) forbids the exclusive use of experimental kinetic reaction parameters and so demands additional methods of estimating them, (ii) prohibits the determination of rate parameters from first principle quantum chemical calculations for each individual reaction, and (iii) favors generic rate estimates for reaction classes rather than detailed estimation of each individual reaction's rate. Furthermore, sophisticated kinetic modeling algorithms for mechanism generation and reduction,[1−3] determination of the model's valid parameter range,[4,5] and model sensitivity analysis[6,7] rely on the accuracy of the rate estimates. Consequently, the rules for rate estimation must be of reasonable accuracy for good model predictions.

For years, conventional transition-state theory has provided the theoretical framework for extrapolation and correlation of experimental reaction rate coefficients to temperatures outside the range of preexisting experimental data and to experimentally unexplored systems.[8−15] Benson and co-workers[8] developed the procedures of thermochemical kinetics and estimated the properties of the transition state using chemical intuition and comparison with stable molecules. In the first paper of this series,[16] we introduced a systematic procedure based on ab initio calculations to predict the thermochemical properties of transition states and arrived at a protocol to predict reaction rates using transition-state theory combined with Benson's group addivity (GA) values. We partitioned the transition-state structures into reactive and unreactive moieties and demonstrated the near constancy of the computed geometrical parameters of the reactive moiety in transition structures within a chosen homologous reaction series. We analyzed the reactive group by assuming that the unreactive moiety contributes equally to

* Corresponding author. E-mail: whgreen@mit.edu. Fax: 001-617-252-1651.

[†] Massachusetts Institute of Technology.

[‡] Present address: Chemical Engineering and Petroleum Refining Department, Colorado School of Mines, 329 Alderson Hall, Golden, Colorado 80401.

10.1021/jp013957c CCC: $22.00
Published on Web 05/08/2002

the thermochemical properties of both the reactant and the transition state. We assigned its contribution to be equal to that of Benson's group values and thereby found that the reactive moiety furnishes a nearly constant and transferable contribution to the free energy of activation. We identified the average contribution from the reactive moiety ("supergroup") as a characteristic property of a given reaction class. We subsequently developed generic rate rules for 15 different families of abstraction reactions.[17]

Although our method worked well for many reaction families, there is no obvious physical basis for our partitioning of the total energy or for assuming the contribution from the unreactive moiety to be equal to its GA value. In the present work, we therefore attempt to understand the quantum mechanical basis for group additivity as observed in the transition states using the atoms in molecule (AIM) treatment of Bader.[18] Bader recently explained[19] why group additivity works for the heats of formation of linear hydrocarbons and silanes by using the quantum mechanics of a proper open system. The AIM energy data for the linear hydrocarbons indicated the presence of two different methyl and three different methylene groups depending upon whether the group is attached to a neighboring CH_3 or a CH_2R group. In other words, AIM analysis of the bond critical points on the charge density surface revealed a much finer classification of groups compared with that of Benson's groups, which are derived semiexperimentally. In the present work, we extend the AIM analysis to branched hydrocarbons and transition structures for $RCH_3 + H \rightarrow RCH_2 + H_2$.

In our earlier work,[16,17] we observed very small but systematic variations (<0.3 kcal/mol) in the enthalpy value for several supergroups with increasing substitution β to the Z- - -H bond being broken (Z = C, O, C(O), C_d, C_t, etc). The variations were so small that we were reluctant to ascribe them to substituent effects. One reason for small substituent effects is that the homologous series considered in our earlier publications involved primarily variations of the alkyl group next to the reaction center. To observe and understand non-next-neighbor substituent effects, one needs to investigate the effect of a wider variety of β substituents, as we have done in the present work.

For α substituents (viz. as in substituted methanes, CH_3X, with regard to our definition of the supergroups), the {C/X/H2/−H/Y} supergroup varies with substituents, X, and it thereby includes steric and electronic effects of X and their impact on the C−H bond strength. Although Benson later introduced correction terms to account for non-next-neighbor interactions (e.g., gauche effect, eclipsing interaction in cis isomers, etc.), neither the group additivity method of Benson nor the way we have derived our supergroups includes any non-next-neighbor effects directly. It is not evident whether the unreactive moiety of substituted systems contributes equally to the reactant and the transition-structure thermochemical value. If such a constant contribution is correct, it would allow us to have fewer reaction classes and would make it simpler to develop a complete set of rate estimation parameters. However, forcing this approximation may mask significant chemical detail. A good method for predicting the generic rate must allow one to incorporate the extreme behaviors of unique and exceptional molecules in any given general class.

In the present work, in addition to the AIM analysis, (i) we intend to determine whether β substituents perturb the thermochemical values of the reactive moiety (supergroup) by extending our previous investigation on hydrogen abstractions from alkanes and by substantially broadening the range of substituents. We study the reaction series $CH_3CH_2X + Y \rightarrow CH_2CH_2X + YH$ with X varying from alkyl to π acceptor (e.g., CH═CH_2, CCH, CHO, $COCH_3$, COOH, $COOCH_3$) to lone pair substituents (e.g., F, NH_2, OH, SH, Cl, OCH_3, OCOH, $OCOCH_3$). (ii) We look for alternate ways of accommodating the effects of substituents on supergroups within the general method of group additivity. (iii) Because the triplet repulsion between Y and C in the transition state is known[20] to influence the activation energy in hydrogen transfer reactions, we investigate abstraction by both H and CH_3 groups. (iv) The effect of multiple substituents on the reaction rate is examined by considering $CH_3CHCl_2 + H \rightarrow CH_2CHCl_2 + H_2$, $CH_3CCl_3 + H \rightarrow CH_2CCl_3 + H_2$, and $(RCH_2)_nCH_{(4-n)} + H$, and (v) the distance dependence of the transmission of electronic effects is considered through $CH_3CH_2CH_2F + H \rightarrow CH_2CH_2CH_2F + H_2$ and $CH_3CH_2CH_2Cl + H \rightarrow CH_2CH_2CH_2Cl + H_2$.

We begin with the AIM analysis of hydrocarbons and transition structures followed by a brief summary of the substituent-dependent conformational preferences in the optimized structures of reactants, transition states, and product radicals. We then discuss the correlation of bond dissociation energies (BDE) and radical stabilization energies (RSE) with barrier height at 0 K. Subsequently, we demonstrate the performance of our procedure and the chosen level of ab initio calculation in predicting the thermochemical properties of stable molecules in comparison to experimental and group additivity values. Such a comparison is essential to verify whether the chosen level of ab initio calculation performs well even for polar systems. Also, one needs to establish the reliability of GA values for the substituents because they are less well-determined. Then we focus on the transition structures and derive the supergroup thermodynamic values to understand the effect of substituents on {C/C/H2/−H/H} and {C/C/H2/−H/C/H3} supergroups. Subsequently, we attempt to correlate the barrier height with the inductive, steric, and hyperconjugative effects of the substituents using a multilinear expression. Instead of using the preestablished group substituent constants,[21−24] we herein use the inductive[22] and steric parameters[23] derived from atomic additivity rules that are based on discrete distance-dependent atomic contributions and are therefore sensitive to conformational differences.

Computational Methodology

In this work, quantum chemical calculations were employed to ascertain the geometric and molecular parameters of transition states, reactants, and products. All calculations were carried out with the Gaussian 98 suite[25] of programs. Calculations were performed using the complete basis set method of Petersson et al.,[26] CBS-Q. Calculations on product radicals and open-shell transition states were done within the unrestricted formalism.

We adopt the commonly used procedure[27] for calculating enthalpies of formation of molecules on the basis of atomization energies and experimental heats of formation ($\Delta_f H_{298}$) for atoms. The enthalpies of formation thus obtained are further improved by incorporating the spin−orbit and bond additivity corrections recommended by Petersson et al.[28]

The total partition function of all species is calculated within the framework of the rigid-rotor harmonic-oscillator approximation with corrections for internal rotations.[29] As described in detail in the first paper[16] of this series, we use MP2/6-31G(d′) optimized geometrical parameters and HF/6-31G(d′) computed harmonic vibrational frequencies scaled by 0.91844 for the calculation of rotational and vibrational partition functions. All torsional motions about single bonds between heavy atoms are treated as hindered internal rotations. The partition functions

for hindered rotations are obtained by solving the Schrödinger equation for energy eigenvalues with the calculated hindrance potential expressed in the form of a Fourier series using the free-rotor basis function. The hindrance potential for the internal rotation is obtained at the HF/6-31G(d′) level by optimizing the $3N - 7$ internal coordinates except the specific dihedral angle that characterizes the torsional motion. This dihedral angle is varied in increments of 30°. The treatment we adopt to obtain hindered-rotor partition functions from the ab initio computed specific hindrance potentials is discussed in detail in our earlier publications[16,17] together with the protocol to derive the supergroup values for the reactive moiety.

A measure of stability of the substituted ethyl radical (CH_2-CH_2X) is derived from the β C−H bond dissociation energy (BDE) of the corresponding substituted ethane (CH_3CH_2X). Radical stabilization energies (RSE) relative to the ethyl radical are inferred from the enthalpy change involved in the isodesmic reaction

$$CH_3CH_3 + \bullet CH_2CH_2X \rightarrow CH_3CH_2\bullet + CH_3CH_2X$$

$$RSE(\bullet CH_2CH_2X) = BDE\ (C_2H_6) - BDE(H\text{- - -}CH_2CH_2X)$$

We used HF/6-31G(d′) wave functions for the AIM energy analysis. The (3, −1) bond critical points in the charge distribution of the molecule are obtained using the EXT94B program.[30] PROAIMV[30] is used to calculate the average energy of an atom by numerical integration of the energy density over the basin of the atom. We used 128 ϕ planes, 96 θ planes, and 192 radial points per integration ray within the sphere.

The group electronegativity of the substituents is calculated using Pauling's electronegativity scale and the "super atom" approximation. The general equation for group electronegativity is given by

$$\chi_g = [V_c E_c + \sum_i N_i E_i]/N$$

wherein V_c and E_c are, respectively, the valence of the central atom and its atomic electronegativity. N_i is the number of bonds of an atom or group, i, connecting to the central atom, and E_i is the atomic or group electronegativity of i (atom or group). N is the sum of the valence of the central atom and the total number of atoms and groups connected to the central atom. The values of atomic electronegativity used in calculating χ_g are H (2.20), C (2.55), N (3.04), O (3.44), F (3.98), S (2.58), and Cl (3.16).

The inductive and steric effect of the substituents are derived using the approach of Galkin and Cherkasov.[21−24] The steric substituent parameter R_s and the inductive substituent constant σ^* are computed at the level of atomic additivity using the following expressions:

$$R_s = 30 \log\left(1 - \sum_{i=1}^{n} \frac{R_i^2}{4r_i^2}\right)$$

$$\sigma^* = \sum_{i=1}^{n} \frac{\sigma_A^i}{r_i^2}$$

R_i is the radius of the ith atom, r_i is the shortest distance between the ith atom of the substituent and the reaction center, n is the number of atoms in the substituent, and σ_A^i is an empirical parameter reflecting the ability of an atom A to attract or donate electrons depending on its chemical nature and valence state.

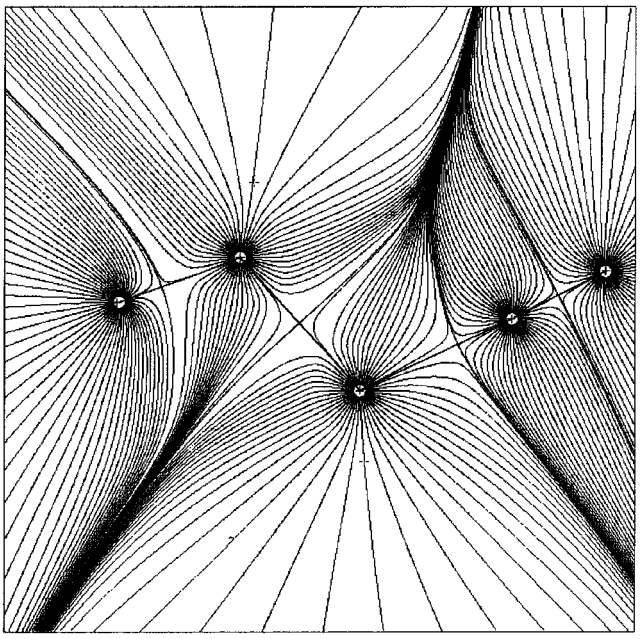

Figure 1. Maps of the gradient vector field of the charge density for the plane containing the abstracting hydrogen and carbons of ethane. Each line represents a trajectory of $\nabla\rho(r)$. The position of the (3, −1) bond critical points in the charge distribution of C- - - H- - - H are denoted by a full circle.

σ_A^i correlates to the difference in electronegativity between atom A and the reaction center, $\Delta\chi_A{}^i$, and the square of the covalent radius of A and is given by $\sigma_A^i = 7.840\ \Delta\chi_A{}^i\ R_A{}^2$. The reaction center in these calculations is taken as the C atom to which the abstracting hydrogen is bonded, so the substituent in these calculations is the entire CH_2X group and not just X. Despite a small electronegative difference between H and C, the inductive effects of all alkyl substituents are taken to be zero, as suggested by Cherkasov for a saturated carbon reaction center.[23] The atomic radii used for these calculations are H (0.37), C (0.77), N (0.75), O (0.73), F (0.71), S (1.04), and Cl (0.99 Å). The calculated R_s and σ^* substituent parameters were shown[21−24] to correlate well with Taft E_s steric ($N = 35$, $R = 0.9854$, $S = 0.141$) and σ constants ($N = 426$, $R = 0.9910$, $S = 0.190$).

Results and Discussion

A. Atoms in Molecule (AIM) Analysis of Transition Structures. In the theory of atoms in molecule[18] (AIM), an atom is defined as a bounded region in real space with boundaries that are determined by the gradient vector field of $\rho(r)$. The gradient of the electron density, $\nabla\rho(r)$, traces gradient paths, which are paths of steepest ascent through $\rho(r)$. Figure 1 displays the gradient vector field of the HF/6-31G(d′) charge density in the molecular plane for the hydrogen abstraction transition structure from ethane by an H atom. An infinite number of paths originating at infinity terminate at a maximum in $\rho(r)$, which practically coincides with a nuclear position that is a (3, −3) critical point on the charge density surface. The set of trajectories that terminates at a given nucleus defines the basin of the atom. In addition to the (3, −3) nuclear critical points, Figure 1 also shows the positions of (3, −1) bond critical points on the forming H---Y and dissociating C---H bonds. The pair of trajectories that, in this plane, terminate at the bond critical points represents the intersection of an interatomic surface with the plane of the Figure. An atomic basin together with its nucleus constitutes an atom. This procedure divides the space into

TABLE 1: Results of Linear Fits of the Total AIM Energy Versus the Number of CH_2 Groups and the Associated Standard Errors in Slope, Intercept, and Energy Values

	slope (au)	intercept (au)	std error in slope (au)	std error in intercept (au)	std error in energy (au)
n-alkanes	−39.03445	−79.22838	8.18×10^{-5}	2.48×10^{-4}	3.42×10^{-4}
n-alkyl TS	−39.03446	−79.68938	6.57×10^{-5}	1.99×10^{-4}	2.75×10^{-4}
isoalkanes	−39.03348	−157.29657	2.24×10^{-4}	6.79×10^{-4}	9.38×10^{-4}
isoS-alkyl TS	−39.03301	−157.75721	6.07×10^{-4}	1.84×10^{-3}	2.54×10^{-3}
isoP-alkyl TS	−39.03361	−157.75778	2.85×10^{-4}	7.81×10^{-4}	6.38×10^{-4}

nonoverlapping atoms. Atomic properties are defined as volume integrals over the atomic basin; for example, the atomic contribution to energy is obtained by integration of the potential energy density.

The reactive moiety consists of two bond critical points corresponding to both the forming (H- - - Y) and the dissociating (C- - - H) bonds. The gross features of the density distribution of the reactive moiety in all transition structures associated with the primary hydrogen abstraction appear very similar; however, there are minor changes in the group boundaries. Because of the transfer of electronic charge between the groups, the positioning of these dividing zero-flux surfaces depends on Y as well as on the groups attached to the reactant carbon. To qualitatively understand the physical origin of group additivity in transition-state-specific groups, we restrict ourselves herein to primary hydrogen abstraction reactions by an H atom (Y = H): $R-CH_3 + H \rightarrow RCH_2\bullet + H_2$ with varying alkyl substituents (i) R = CH_3, C_2H_5, *n*-C_3H_7, *n*-C_4H_9, *n*-C_5H_{11}, and *n*-C_6H_{13}; (ii) R = *i*-C_3H_7, sec-C_4H_9, 2-C_5H_{11}, 2-C_6H_{13}, 2-C_7H_{15}, and 2-C_8H_{17}; (iii) R = $(CH_3)_2CHCH_2$, $(CH_3)_2CHCH_2CH2$, $(CH_3)_2CHCH_2CH_2CH_2$, and $(CH_3)_2CHCH_2CH_2CH_2CH_2$; and (iv) R = $(CH_3)_3C$ and $(CH_3)_2CCH_2CH_3$. Because we have investigated only two members in series (iv), the rest of the discussion will be focused mainly on the first three series and are referred to hereafter as *n*-alkyl, isoS-alkyls, and isoP-alkyls. All the members in a given series differ from each other with respect to the number of methylene groups. In series (ii), the hydrogen being abstracted (bold) is attached to a carbon whose neighboring carbon is a tertiary carbon (viz., $(C\mathbf{H}_3)_2CH(CH_2)_n$-$CH_3$), whereas in series (iii), the neighboring carbon is a secondary carbon (viz., $(CH_3)_2CH(CH_2)_nC\mathbf{H}_3$).

The AIM energy of each atom, $E(\omega)$, in the transition structure is calculated by numerically integrating the energy density. The integration error involved in the calculated total energy ($\Sigma E(\omega) - E$) is on the order of few millihartrees. The difference in $E(\omega)$ compared to its energy in the isolated case, $E^{\infty}(\omega)$, suggests that there is a rearrangement of charge density between the atoms when they are brought together to form a bond. Plots of total AIM energy of the unbranched and branched hydrocarbons, as well as the energy of their transition structures, versus the number of CH_2 groups revealed linear relationships. The fit parameters obtained from linear fits are tabulated in Table 1 along with the standard errors. These linear relationships in energy suggest that there is an exchange of nearly equal and opposite amounts of charge/energy density between the groups separated by the zero-flux surface.

The intercept for each of the equations corresponds to the energy of the first member of each series, $n = 0$, (viz., ethane and *tert*-butane), and it fits to the calculated energy for ethane and *tert*-butane within 0.0002 and 0.001 au, respectively. Thus, the intercepts of the reactant series correspond to the energy of two methyl groups and the energy of a methyl and an isopropyl group:

$$\text{Intercept (i)} = 2E(CH_3)$$

$$\text{Intercept (ii)} = E(CH_3) + E(CH(CH_3)_2)$$

The slope gives the average energy of the CH_2 group. In series (i), there are three types of methylene groups (viz., the methylene group flanked by (1) 2 methylene groups, (2) a methylene and a methyl group, and (3) two methyl groups). In series (ii), one still has the (1) and (2) types of methylene, but the third type is different and is now flanked by a methyl and an isopropyl group. Consequently, if the data set is too small, one can see variations in the slope, which is essentially because the lower members of the homologous series are unique. However, one can anticipate that the inclusion of significantly larger systems in the study would result in the same slope for both of the reactant series, with the lower members of the series deviating slightly from the straight line.

Similar to the intercepts for the reactants, the intercepts for the three families of transition-state structures correspond to the sum of the {C/C/H2/−H/H} supergroup, with the methyl, isopropyl, and isopropyl groups, respectively. They fit to the energy of the transition structures (viz., CH_3CH_2- - -H- - -H and $(CH_3)_2CHCH_2$- - -H- - -H) within 0.0001 and 0.001 au, respectively.

$$\text{InterceptTS(i)} = E(\text{CH3}) + E(\text{C/C/H2/}-\text{H/H})$$

$$\text{InterceptTS(ii)} = E(\text{CH(CH3)2}) + E(\text{C/C/H2/}-\text{H/H})$$

$$\text{InterceptTS(iii)} = E(\text{CH(CH3)2}) + E(\text{C/C/H2/}-\text{H/H})$$

Subsequently, the differences in the intercept for the corresponding equations of the transition structure and the reactant in all three series amount to

$$\text{InterceptTS(i)} - \text{Intercept(i)} = \{E(\text{CH3})^{\text{TS}} - E(\text{CH3})^{\text{R}}\} + [E(\text{C/C/H2/}-\text{H/H}) - E(\text{CH3})^{\text{R}}] = -0.4610 \text{ au}$$

$$\text{InterceptTS(ii)} - \text{Intercept(ii)} = \{E(i\text{-pr})^{\text{TS}} - E(i\text{-pr})^{\text{R}}\} + [E(\text{C/C/H2/}-\text{H/H}) - E(\text{CH3})^{\text{R}}] = -0.4606 \text{ au}$$

$$\text{InterceptTS(iii)} - \text{Intercept(iii)} = \{E(i\text{-pr})^{\text{TS}} - E(i\text{-pr})^{\text{R}}\} + [E(\text{C/C/H2/}-\text{H/H}) - E(\text{CH3})^{\text{R}}] = -0.4612 \text{ au}$$

For the $n = 0$ case, the terms within {} and [] correspond, respectively, to the unreactive and the reactive moiety contributions to the barrier height. For the three series, the sum of the differences remains nearly the same. Also, the slope of the reactant and transition-state energies are nearly the same within the level of accuracy of the calculation, which suggests a nearly constant contribution from the $(CH_2)_n$ chains and hence a constant $[E(\text{C/C/H2/}-\text{H/H}) - E(\text{CH3})^{\text{R}}]$ value for all values of *n*. However, if one simply computes the AIM energy of either the $[E(\text{C/C/H2/}-\text{H/H}) - E(\text{CH3})^{\text{R}}]$ term or the term within curly brackets, one will observe that these quantities vary significantly from molecule to molecule. The problem is that the AIM energy of any group is quite sensitive to the details of the charge density distribution, so the energy is not very transferable. Consequently,

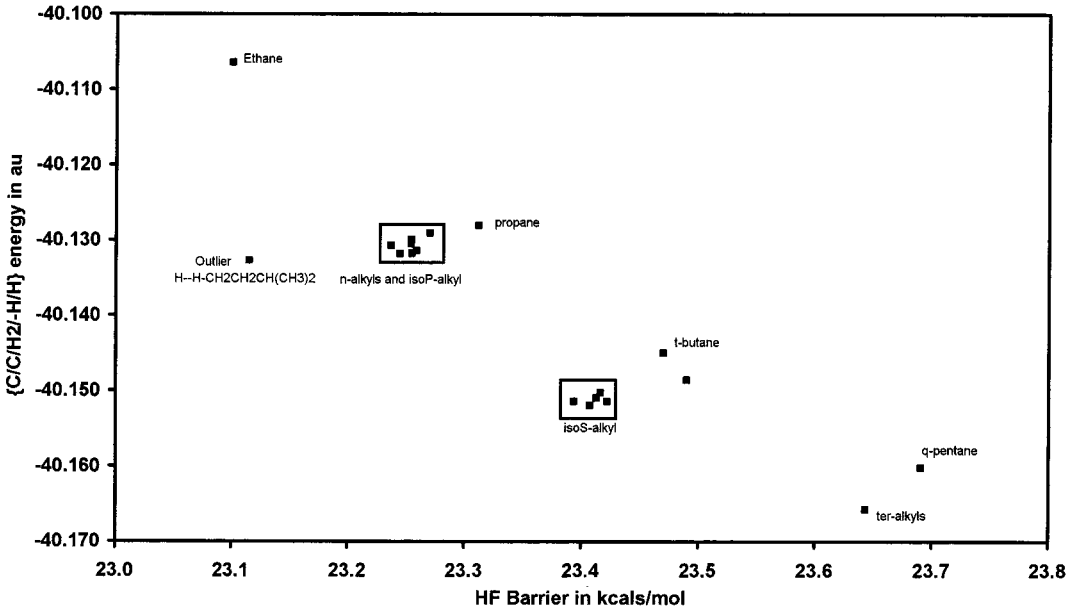

Figure 2. Plot of atoms in molecule (AIM) energy (au) of the supergroup {C/C/H2/−H/H} vs the HF/6-31G(d′) barrier height (kcal/mol) for the primary hydrogen abstraction transition structures of linear and branched hydrocarbons.

when deriving groups from quantum chemical calculations, which are transferable from one molecule to another, one needs the average energy of a group. In this regard, it is justifiable to use the GA energy for the unreactive moiety because groups are derived from a best-fit procedure to all the molecules and from experimental heat of formation values.

It is important to realize that we do not force the methyl groups of ethane, propane, *tert*-butane and neopentane to have the same value either in the rectants or in the TS. Although each methyl group has a different AIM energy, the change in that energy in going from reactants to the TS is nearly constant. Figure 2 is a plot of AIM energy of the TS supergroup {C/C/H2/-H/H} versus the HF/6-31G(d′) barrier height for all 23 of the reactions considered in this analysis. The supergroup energy falls into four different classes depending upon the nature of the neighboring carbon atom (viz., CH_3, primary, secondary, or tertiary (the first member of series (iii) is an outlier)). It is interesting to note that the energy of the supergroups derived from the isoP-alkyl series, (iii), differs from that of the isoS-alkyl series, (ii), and that the former is similar to that of the *n*-alkyl series, (i). The transition structures of both series (i) and (iii) are of the same type H---HCH2CH2R; the only difference is that the former has a straight chain R whereas the latter has branching at the end. Thus, the quantum mechanical analysis of group additivity on the basis of charge density demonstrates non- next-neighbor effects that are ignored by conventional group additivity.

In our earlier work, the bond strength of the abstracting X- - -H bond varied parallel with the barrier height or the ΔH^{298} values of the supergroups, and we ascribed this variation to the stabilization provided by the given substituent in the resulting product radical. Herein, using the AIM approach, we would like to see the correlation, if any, between the stabilization energy of the reactive moiety carbon atom (−CH2- - - H- - - H) in the transition state and the barrier height. We define the stabilization energy (SE) as the difference in energy between any given isolated atom (the energy of which is defined merely by its atom potential) and the same atom in the molecule under consideration (the energy of which is defined by other atoms in the molecule). We calculated the stabilization energy of the reactive moiety C, which is abstracting H and the hydrogen that is being abstracted in the transition structures of primary hydrogen abstraction by H. Figure 3 is a plot of stabilization energy of the reactive moiety C atom versus the HF barrier height. Except for the first members of each series, the SE of the C atom in the TS is nearly the same along the series. If one considers the series ethane → propane → *tert*-butane → neopentane, the barrier height correlates with the SE of the reactive moiety C, and at the low level of theory, HF/6-31G(d′), the barrier height seems to increase with β-alkyl substitution (Figure 3). However, at the CBS-Q level, with the inclusion of corrections for omitted electron correlation and an incomplete basis set, the barrier height slightly decreases with β-alkyl substitution[16,17] (ethane 9.73, propane 9.82, *tert*-butane 9.63, neopentane 9.77 kcal/mol). The transition structure from isopentane, H- - -H—CH_2CH_2CH-$(CH_3)_2$, is an outlier, and it has a low barrier height. A similar clustering pattern is observed in the plot of stabilization energy of the abstracting H atom or the migrating H atom versus the barrier height (Supporting Information).

The present work is consistent with Bader's conclusion that the transferability of group values (e.g., ΔH_f^{298K}) is a result of compensatory transferability wherein the change in the properties of one group are compensated for by equal but opposite changes in the properties of the adjoining group. Thus, to first order, the analysis based on charge density qualitatively explains the constancy of the supergroup energy value. The existence of two bond critical points on the CH_2- - -H- - -H moiety allows for further splitting of supergroups into three transition-state-specific groups. Though it is not shown here, this analysis gives the qualitative rationale for subdividing the central {−H/C/H} group into {−H/C^p/H}, {−H/C^s/H}, and {−H/C^t/H} because the bond critical points are expected to shift along with the change in the charge density for 1, 2, and 3 °C. The AIM analysis also suggests a division of the {C/C/H2/−H/H} group into three subgroups: {C/C^p/H2/−H/H}, {C/C^s/H2/−H/H}, and {C/C^t/H2/−H/H}. However, the barrier heights for the test sets in refs 16 and 17 with alkyl substituents vary only by 0.5 kcal/mol. It is therefore a good approximation to treat them as a single group, using the average value as the best guess.

B. Geometries of Stable Molecules, Transition Structures, and Radicals. Before discussing the calculated BDE or the RSE associated with the substituted ethyl radicals and thermochemical

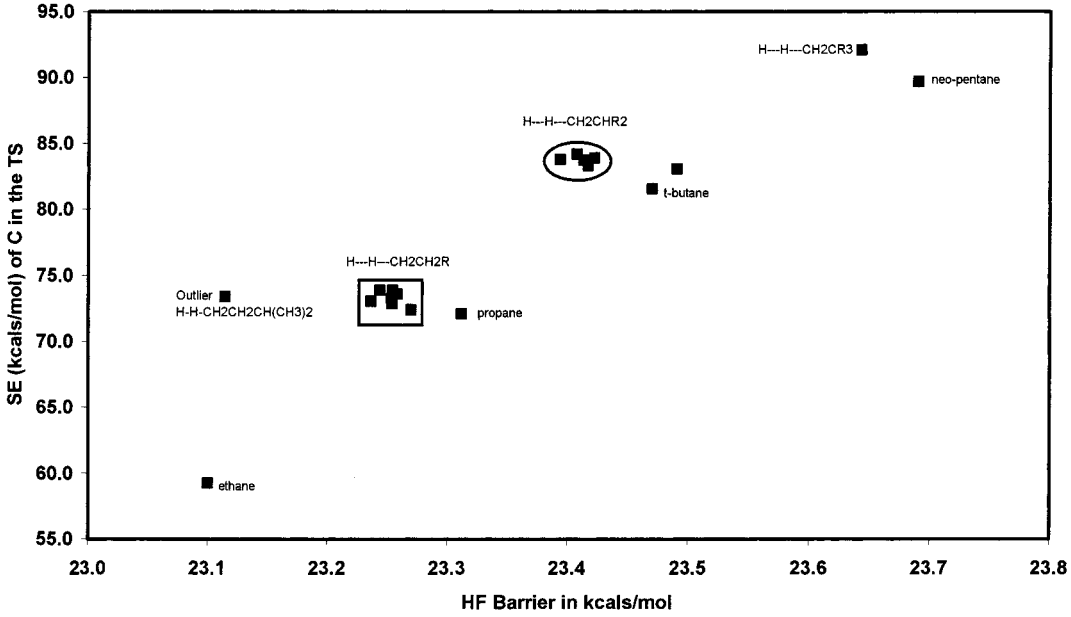

Figure 3. Plot of stabilization energy (kcal/mol) of the reactive moiety carbon in the transition structures of primary hydrogen abstraction from alkanes by H vs the barrier height (kcal/mol).

properties of stable molecules, it is useful to examine the general features of the geometries of substituted ethane (XCH_2CH_3) and ethyl ($XCH_2CH_2\bullet$) radicals together with those of transition structures. The MP2/6-31G(d′) optimized Cartesian coordinates of reactants and transition states are provided in Tables S1 and S2, respectively, of the Supporting Information whereas the unscaled harmonic frequencies of the transition structures and reactants computed at the HF/6-31G(d′) level are listed in Tables S3 and S4, respectively. For well-known reasons,[31] all substituted ethanes prefer a staggered conformation around the CH_3- - - CH_2X (τ_{HCCX} = 180.0) bond. The second torsional mode with lone pair substituents such as OH, SH, NH_2, OCH_3, OC(O)H, and $OC(O)CH_3$ exhibits minima at both the gauche (CC- - - ZW = ∼60°) and anti (CC- - - ZW = 180°) conformations (Z = O, N, S; W = H or C) with the latter being energetically favored in all cases except for the SH group. The reported relative abundance of the trans and gauche conformers of ethyl methyl ether in the gas phase at 20 °C from gas electron diffraction studies[32] is $n_t/(n_t + n_g) = 0.80 \pm 0.08$, which is consistent with our calculations.

In the case of ethyl esters (X = OC(O)H and $OC(O)CH_3$), the third hindrance potential around the O- - -C(O) bond prefers a synperiplanar conformation (CO- --C═O = 0°) over the antiperiplanar conformation by ∼4.6 kcal/mol. However, the anti conformation is also a minimum on the potential energy surface. In all cases with a carbonyl group in the substituents, the bonds in the β position with respect to the carbonyl group (τ_{HCCO} = 0° in C**H**$_3$CO- - - substituents) prefer an eclipsed conformation with C═O functionality in accordance with earlier findings.[33] However, the origin of stabilization of the eclipsed conformer is still not clear.[34] In the present work, we concentrate only on the lowest-energy conformer while computing the thermochemical properties and barrier heights.

Similar to substituted methyl radicals,[35] ethyl radicals with lone pair substituents adopt a slightly nonplanar radical center (CH_AH_BC = 162−165°) even with multiple β (e.g., CH_2CHCl_2 and CH_2CCl_3) and γ substituents (e.g., $CH_2CH_2CH_2Cl$ and CH_2-CH_2CH_2F). Ethyl radicals with carbonyl π-acceptor β substituents prefer a nearly planar radical center (CH_AH_BC = 177−179°) whereas those with CH═CH_2 and CCH β substituents assume a nonplanar radical center (CH_AH_BC = 165°). The preferred hybridization at the radical center is a consequence of the effective interaction between either the π or the n orbital of X with the radical center, 2p(C•). In $XCH_2CH_2\bullet$, the hybridization is largely due to the hyperconjugative interaction of the radical center with its β bonds, owing to the intervening CH_2 group. The latter does not allow for mesomeric interactions between X and the reaction center. Consequently, it allows for two possible orientations for the CH_2•- - - CH_2X bond with either (1) the β-C−X bond being antiperiplanar to the 2p(C•) orbital ($H_ACCX \approx 90°$ and $H_BCCX \approx -90°$) or (2) one of the β-C−H bonds being antiperiplanar to the 2p(C•) orbital ($H_ACCX \approx 30°$ and $H_BCCX \approx -160°$). The latter is largely favored by π-acceptor substituents (X = CHO, $COCH_3$, COOH, $COOCH_3$, CH═CH_2, CCH) and lone pair substituents from second-row atoms such as F, NH_2, OH, OCH_3, OC(O)H, and $OC(O)CH_3$ and alkyl substituents. Nevertheless, the third-row substituents Cl and SH favor the former. Results are summarized in Figure 4 using the simple Newman projection diagrams. The CBS-Q energies of both conformers of all substituted ethyl radicals are tabulated in Table 2. Complete optimization of conformer (2) with β-C−H hyperconjugative interaction results in conformer (1) if X = Cl and SH whereas the opposite is the case for OH, OCH_3, and NH_2 substituents.

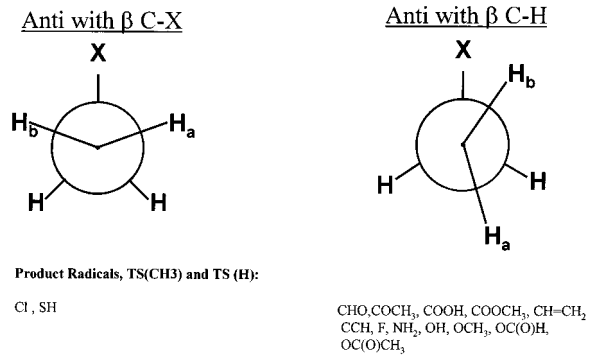

Figure 4. Newman projection diagrams listing the preferred conformation around the CH_2X- --$CH_2(HY)$ bond in transition structures for reactions with H and CH_3 as well as in product radicals.

TABLE 2: CBS-Q Energies and Energy Differences of Conformers of Transition Structures and Product Radicals Involved in H Abstraction Reactions from CH_3CH_2X by H Atoms and CH_3 Radicals

	E(TS) (au), XCH_2CH_2—H—H			E(product radical) (au), XCH_2CH_2•		
substituent, X	β C—H gauche	β C—X anti	ΔE (kcal/mol)	β-C—H	β-C—X	ΔE (kcal/mol)
CH_2Cl	−539.271303	−539.272258	0.599	reverted	−538.129444	
CH_2SH	−477.862111	−477.863307	0.750	reverted	−426.720069	
CH_2OH	−155.251832	−155.250684	−0.720	−154.107476	reverted	
CH_2OCH_3	−194.463095	−194.462068	−0.644	−193.328695	reverted	
$CH_2OC(O)H$	−268.449229	−268.448423	−0.505	−267.304913	−267.304075	−0.525
$CH_2OC(O)CH_3$	−307.687349	−307.686335	−0.636	−306.542855	−306.541918	−0.588
CH_2CHO	−193.289698	−193.289177	−0.326	−192.146595	−192.144323	−1.426
CH_2COCH_3	−232.528116	−232.527646	−0.295	−231.384496	−231.382310	−1.372
CH_2COOH	−268.472241	−268.471656	−0.367	−267.328827	−267.326451	−1.490
CH_2COOCH_3	−307.684035	−307.683451	−0.366	−306.540451	−306.537978	−1.552
CH_2NH_2	−135.379122	−135.377380	−1.093	−134.234489	reverted	
CH_2F	−179.274771	−179.274380	−0.245	−178.130704	−178.130178	−0.330
CH_2CHCH_2	−157.354258	−157.354191	−0.042			
CH_2CCH	−156.129683	−156.129627	−0.035	−154.985561	−154.984554	−0.632

	E(TS) (au), XCH_2CH_2—H—CH_3		
substituent, X	β C—H gauche	β C—X anti	ΔE (kcal/mol)
CH_2Cl	−578.511909	−578.512690	0.490
CH_2SH	−517.100875	−517.102075	0.753
CH_2OH	−194.490251	−194.489715	−0.336
CH_2OCH_3	−233.702284	−233.701282	−0.629
$CH_2OC(O)H$	−307.688966	−307.688209	−0.475
$CH_2OC(O)CH_3$	−346.926892	−346.926200	−0.434
CH_2CHO	−232.529196	−232.528046	−0.722
CH_2COCH_3	−271.767592	−271.766559	−0.648
CH_2COOH	−307.711946	−307.710768	−0.739
CH_2COOCH_3	−346.923551	−346.922681	−0.546
CH_2NH_2	−174.617179	−174.615993	−0.744

Problems were encountered while optimizing the structures of but-1-ene-3-yl and $CHCl_2$ radicals at the MP2/6-31G(d′) level, and our attempts to obtain the CBS-Q energy of these radicals proved futile. A similar problem was reported earlier for CH_2═$CHCH_2CH_2$• by Smith et al.[36] In the present work, we optimized the structure of the but-1-ene-3-yl radical at the B3LYP/6-31G(d′) level and computed its energy at the CBS-QB3 level. The C—H BDE of CH_2═$CHCH_2CH_3$ in Table 4 is reported at the CBS-QB3 level.

Similar to that of the product radical, the preferred conformation around XCH_2- - -$CH_2(HY)$ (with Y = H or CH_3) in the transition structure depends on the nature of the substituent, X. The possible preferred conformations are similar to those discussed for the radicals except that the relative orientation of X in the transition structures is with respect to the C- - - -H bond that is being broken (i.e., the nascent radical orbital instead of the established radical orbital 2p(C•)). The favored conformation, with both H and CH_3 as the abstracting radical, is the gauche form ($\tau_{H---CCX} \approx 60°$) in almost all cases except for Cl and SH substituents for which the anti form ($\tau_{H---CCX} \approx 180°$) is found to be more stable. In other words, the preferred relative orientation in the transition structure parallels that of the resulting product radical. The CBS-Q energies for the anti and gauche forms of transition structures are listed in Table 2 along with those of the resulting substituted ethyl radicals. The relative energy difference between these two conformers of transition structures at the CBS-Q level is typically within 1 kcal/mol whereas the barrier for the hindered rotation around this bond is between 3.2 and 5.8 kcal/mol depending upon X.

The optimized geometrical parameters of the reactive moiety, CH_2- - -H- - - Y, are tabulated in Table 3 along with the magnitudes of the imaginary frequency corresponding to the reaction coordinate and the expectation values of the spin operator for the unrestricted wave function. Besides the differences observed in the conformational preference of X, Table 3 also reveals small fluctuations in the reactive moiety. Interestingly, the geometry of the reactive moiety remains nearly the same for the following substituent pairs: (OC(O)H, $OC(O)CH_3$); (CHO, $COCH_3$); and (COOH, $COOCH_3$). These are pairs

TABLE 3: MP2/6-31G(d′) Optimized Geometrical Parameters of the Reactive Moiety in the Transition Structures of Substituted Ethanes and the Magnitudes of the Imaginary Frequency Corresponding to the Reaction Coordinate[a]

transition structure	C—H (Å)	H—Y (Å)	C—H—X (deg)	$\langle S^2 \rangle$	ν (cm^{-1})	barrier
$C_2H_6 + H$	1.409	0.891	178.1	0.788	2227	9.73
$CH_3CH_2F + H$	1.419	0.882	178.5	0.788	2266	11.28
$C_2H_5NH_2 + H$	1.413	0.892	177.9	0.788	2206	9.68
$C_2H_5OH + H$	1.414	0.892	177.9	0.789	2211	10.14
$C_2H_5OCH_3 + H$	1.418	0.883	178.1	0.788	2245	10.66
$C_2H_5OC(O)H + H$	1.418	0.882	178.3	0.788	2264	11.03
$C_2H_5OC(O)CH_3$	1.418	0.882	178.7	0.788	2258	10.81
$C_2H_5Cl + H$	1.413	0.889	179.5	0.788	2289	10.68
$C_2H_5SH + H$	1.408	0.893	179.7	0.788	2264	9.38
$C_2H_5CHO + H$	1.412	0.886	178.8	0.788	2261	10.75
$C_2H_5C(O)CH_3$	1.411	0.888	178.9	0.788	2249	10.45
$C_2H_5COOH + H$	1.412	0.886	178.7	0.789	2262	10.91
$C_2H_5C(O)OCH_3$	1.412	0.887	178.7	0.788	2256	10.72
C_2H_5CH═$CH_2 + H$	1.414	0.888	178.4	0.788	2227	9.94
$C_2H_5CCH + H$	1.420	0.884	177.9	0.788	2256	10.54
$CCl_2HCH_3 + H$	1.421	0.879	178.8	0.788	2316	11.06
$CCl_3CH_3 + H$	1.418	0.913	174.7	0.788	2333	11.60
$CH_3CH_2CH_2Cl + H$	1.411	0.886	178.6	0.788	2269	9.99
$CH_3CH_2CH_2F + H$	1.411	0.887	178.4	0.788	2265	10.22
$C_2H_6 + CH_3$	1.316	1.355	177.6	0.789	2544	14.09
$C_2H_5Cl + CH_3$	1.324	1.349	179.6	0.789	2542	13.32
$C_2H_5OH + CH_3$	1.32	1.357	177.6	0.789	2532	14.05
$C_2H_5NH_2 + CH_3$	1.318	1.357	178.0	0.789	2537	13.81
$C_2H_5SH + CH_3$	1.319	1.355	179.4	0.789	2544	13.06
$C_2H_5CHO + CH_3$	1.326	1.343	178.3	0.790	2551	13.65
$C_2H_5COOH + CH_3$	1.324	1.341	176.5	0.789	2555	13.64
$C_2H_5OCH_3 + CH_3$	1.326	1.339	175.1	0.789	2549	14.08
$C_2H_5OC(O)H + CH_3$	1.328	1.337	176.5	0.789	2550	14.11
$C_2H_5C(O)CH_3 + CH_3$	1.324	1.345	178.4	0.789	2551	13.39
C_2H_5CH═$CH_2 + CH_3$	1.322	1.348	177.1	0.792	2543	13.73
$C_2H_5OC(O)CH_3 + CH_3$	1.326	1.339	176.1	0.789	2550	14.44
$C_2H_5C(O)OCH_3 + CH_3$	1.324	1.342	176.1	0.789	2554	13.57

[a] CBS-Q 0 K ZPE corrected barrier heights are in kcal/mol.

TABLE 4: CBS-Q Level Calculated BDEs, Heats of Reaction, and Radical Stabilization Energies for the Reactions Investigated in This Study

reaction	BDE at 0 K (kcal/mol)	ΔH_R by H at 0 K (kcal/mol)	ΔH_R by CH_3 at 0 K (kcal/mol)	RSE at 0 K (kcal/mol)
$H_2 \rightarrow H + H$	104.45			
$CH_4 \rightarrow CH_3 + H$	103.73	−0.72		
$C_2H_6 \rightarrow C_2H_5 + H$	99.95	−4.50	−3.78	
$C_3H_8 \rightarrow n\text{-}C_3H_7 + H$	100.32	−4.13	−3.41	
$t\text{-}C_4H_{10} \rightarrow$ iso-$C_4H_9(1) + H$	101.05	−3.40	−2.68	
Neo-$C_5H_{12} \rightarrow$ q-$C_5H_{11} + H$	101.67	−2.78	−2.06	
$C_2H_5NH_2 \rightarrow CH_2CH_2NH_2 + H$	100.66	−3.79	−3.07	−0.71
$C_2H_5OH \rightarrow CH_2CH_2OH + H$	100.96	−3.49	−2.77	−1.01
$C_2H_5F \rightarrow CH_2CH_2F + H$	101.91	−2.54	−1.82	−1.96
$C_2H_5OCH_3 \rightarrow CH_2CH_2OCH_3 + H$	101.62	−2.83	−2.11	−1.67
$C_2H_5OC(O)H \rightarrow CH_2CH_2OC(O)H + H$	101.82	−2.63	−1.91	−1.87
$C_2H_5OC(O)CH_3 \rightarrow CH_2CH_2OC(O)CH_3 + H$	101.71	−2.74	−2.02	−1.76
$C_2H_5SH \rightarrow CH_2CH_2SH + H$	99.49	−4.95	−4.24	0.46
$C_2H_5Cl \rightarrow CH_2CH_2Cl + H$	100.52	−3.93	−3.21	−0.57
$C_2H_5CHO \rightarrow CH_2CH_2CHO + H$	100.45	−4.00	−3.28	−0.50
$C_2H_5COCH_3 \rightarrow CH_2CH_2COCH_3 + H$	100.50	−3.95	−3.23	−0.55
$C_2H_5COOH \rightarrow CH_2CH_2COOH + H$	100.76	−3.69	−2.97	−0.81
$C_2H_5COOCH_3 \rightarrow CH_2CH_2COOCH_3 + H$	100.68	−3.77	−3.05	−0.73
$C_2H_5CH{=}CH_2 \rightarrow CH_2CH_2CH{=}CH_2 + H$	100.48	−3.97	−3.25	−0.53
$C_2H_5CCH \rightarrow CH_2CH_2CCH + H$	101.17	−3.28	−2.56	−1.22
$C_2H_5CHCl2 \rightarrow CH_2CH_2CHCl_2 + H$	101.44	−3.01	−2.29	−1.49
$C_2H_5CCl_3 \rightarrow CH_2CH_2CCl_3 + H$	102.84	−1.61	−0.89	−2.89
$C_2H_5CH_2F \rightarrow CH_2CH_2CH_2F + H$	100.48	−3.97	−3.25	−0.53
$C_2H_5CH_2Cl \rightarrow CH_2CH_2CH_2Cl + H$	100.48	−1.61	−3.25	−0.53

with similar electronic effects of X but with different bulkiness parameters of X. In combination with our earlier work,[16,17] wherein the substituents are alkyl groups of varied bulkiness, these results suggest that the supergroups are not very sensitive to the bulkiness of the β substituents. As shown below, this similarity in reactive moiety geometry corresponds to nearly identical S and $C_p(T)$ values for the supergroup. Our general conclusion is that γ-alkyl substitutions that modify only the sterics generally have little effect on reaction rates.

C. Bond Dissociation Energies and Radical Stabilization Energies. Bond dissociation energies for C−H bonds β to the substituent in substituted ethanes are tabulated in Table 4 together with the radical stabilization energies (RSE). Negative RSE as defined by eq 3 indicates that the radical CH_2CH_2X is destabilized with respect to $CH_3CH_2\bullet$, thus resulting in a larger C−H BDE in CH_3CH_2X than in CH_3CH_3. As can be seen from Table 4, all substituents investigated in this study tend to destabilize the $CH_3CH_2\bullet$ radical. The only exception is SH. This result is in contrast to findings for CH_2X[35] radicals, in which the same X substituents are shown to stabilize the methyl radical. The C−H bond strength varies by ∼2.4 kcal/mol among the $XCH_2CH_2\bullet$ systems and is at its maximum for F (101.9 kcal/mol) and at its minimum (99.5 kcal/mol) for SH. The barrier height for H abstraction varies by ∼1.9 kcal/mol and is, in fact, smaller in the case of SH and larger in the case of F compared to that of unsubstituted ethane. Increasing Cl substitution progressively increases the β-C−H bond strength, thus suggesting the electronic influence of the electronegative Cl atom. Every additional Cl increases the C−H bond strength by nearly 1 kcal/mol. In contrast, the C−H bond strengths (γ position) in propyl chloride and propyl fluoride are nearly the same as in the unsubstituted propane, which is in agreement with the expectation that the electronic or "through-bond" influence of the electronegative substituent decreases with the increasing number of the intervening bonds. However, neither the BDE nor the RSE is found to correlate linearly with the barrier height (Figure 5). One can see that the bond strength is the same within 0.1 kcal/mol for the following pairs of substituents—(OCOH, $OC(O)CH_3$); (CHO, $COCH_3$); and (COOH, $COOCH_3$)—whereas the barrier heights vary roughly by 0.3 kcal/mol, which suggests

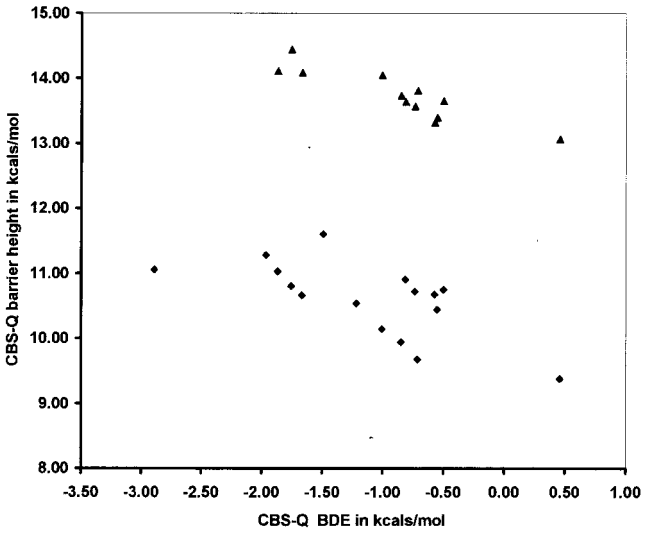

Figure 5. Plot of CBS-Q bond dissociation energy (kcal/mol) for the C−H bond vs its abstraction barrier height (kcal/mol) at the CBS-Q level. The filled squares correspond to abstraction by H , and the filled triangles correspond to abstraction by a methyl group.

that the barrier height and, in turn, the H^{298} of the supergroups is a function of both the *electronic* and *steric* effects of the substituents.

D. Thermochemical Properties of Stable Molecules. Our results for the thermochemical properties of substituted ethanes are given in Tables 5 and 6 together with GA-based predictions and data from the literature. Although there are many available thermochemical databases, we herein restrict ourselves to the Web-based NIST database[37] wherever possible. Because experimental data are not available in the NIST Webbook for 11 of the 18 substituted systems considered in the present study, we also refer to the earlier compilation by Stull, Westrum, and Silke[38] (SWS).

The CBS-Q predictions for S and $C_p(T)$ values are in good agreement with the literature and GA values for butene, butyne, ethanol, thioethanol, aminoethane, propanal, and butanone. In general, the calculated entropy is smaller than the experimental

TABLE 5: Comparison of Calculated Thermodynamic Properties of C_2H_5X with Literature Values

species	method	$\Delta_f H_{298}$ (kcal/mol)	S^{298} (cal/mol K)	C_p^{300} (cal/mol K)	C_p^{400} (cal/mol K)	C_p^{500} (cal/mol K)	C_p^{600} (cal/mol K)	C_p^{800} (cal/mol K)	C_p^{1000} (cal/mol K)	C_p^{1500} (cal/mol K)
CH_3CH_2CHO	ab initio	−44.51	72.68	19.70	22.95	26.32	29.45	34.71	38.75	45.05
	SWS	−45.90	72.83	18.87	23.09	26.89	30.22	35.45	39.27	
	GA (Benson)	−44.30	72.62	19.43	23.42	26.94	29.99	35.34	39.18	
	therm	−44.50	72.73	19.42	23.41	26.92	29.97	35.32	39.17	
	NIST	−45.09	72.75	19.35	23.04	26.98	30.71	37.09	42.14	50.60
$CH_3CH_2C(O)CH_3$	ab initio	−57.61	80.46	24.74	29.71	34.42	38.64	45.58	50.88	59.15
	SWS	−56.97	80.81	24.68	29.81	34.76	39.09	46.08	51.33	
	GA(Benson)	−56.68	80.94	24.22	29.76	34.64	38.88	46.06	51.35	
	therm	−56.88	81.06	24.17	29.70	34.59	38.84	46.03	51.35	
	NIST	−57.02	81.10	24.40	29.73	34.67	38.99	45.95	51.15	59.08
C_2H_5COOH	ab initio	−108.37	77.26	21.79	26.23	30.45	34.20	40.35	44.98	51.78
	GA(Benson)	−108.40	77.02	22.23	27.32	31.24	34.59	40.24	44.18	
	therm	−108.60	72.37	22.29	27.24	31.30	34.61	40.19	44.13	
	NIST	−107.00	77.10							
$CH_3CH_2COOCH_3$	ab initio	−105.29	85.73	26.88	32.21	37.54	42.38	50.43	56.61	65.93
	GA(Benson)	−103.48	89.14							
	therm	−102.79	84.49	28.59	34.39	39.50	43.94	51.34	56.90	
	NIST	−103.00	0.00	0.00	0.00	0.00	0.00	0.00	0.00	0.00
$CH_3CH_2OCH_3$	ab initio	−52.20	73.10	22.39	26.84	31.04	34.85	41.24	46.18	53.94
	SWS	−51.73	74.24	21.53	26.08	30.53	34.58	41.19	46.18	
	GA(Benson)	−51.38	74.82	20.81	26.31	30.84	34.81	41.57	46.48	
	therm	−51.60	74.93	20.77	26.23	30.80	34.81	41.56	46.47	
	NIST	−51.73	74.20	22.39	27.22	31.71	35.63	41.96	46.75	54.24
$CH_3OC(O)H$	ab initio	−85.87	68.62	15.56	18.50	21.60	24.51	29.37	32.89	37.59
	SWS	−83.60	72.00	16.00	19.50	22.60	25.20	29.10	32.00	
	GA(Benson)	−85.28	71.53							
	therm	−85.30	71.53	17.13	20.02	22.82	25.31	29.55	32.77	
	NIST	−86.60	68.18	15.44	18.54	21.58	24.28	28.57	31.71	36.44
$CH_3CH_2OC(O)H$	ab initio	−93.89	77.32	21.17	25.75	30.30	34.41	41.01	45.74	52.16
	GA(Benson)	−93.30	81.22							
	therm	−92.59	81.33	22.12	26.87	31.12	34.74	40.65	45.10	
	expt		78.04	21.68	26.35	30.94	35.03	41.57	46.21	52.47
	NIST	−95.20								
$CH_3OC(O)CH_3$	ab initio	−98.71	76.70	20.52	24.87	29.15	33.02	39.45	44.40	51.76
	GA(Benson)	−98.36	79.65							
	therm	−98.38	79.65	22.39	26.69	30.80	34.44	40.24	44.70	
	NIST	−98.00	77.53	20.64	25.17	29.49	33.28	39.31	43.75	50.51
$CH_3CH_2OC(O)CH_3$	ab initio	−107.99	85.69	26.11	32.09	37.79	42.84	51.07	57.28	66.41
	SWS	−105.86	86.70	27.24	32.84	38.70	43.65	51.01	56.05	
	GA(Benson)	−106.38	89.34							
	therm	−105.67	84.69	27.38	33.54	39.10	43.87	51.34	57.03	
	NIST	−106.43	86.70	27.24	32.84	38.70	43.65	51.01	56.05	0.00

value, which is largely due to the consideration of a single conformer in our theoretical calculations. However, we see a significant difference in the calculated entropy of butyne, thus suggesting appreciable errors in the calculated low frequencies of the CCH group. NIST-tabulated $C_p(T)$ values for propanal and ethyl methyl ether show large deviations from GA, ab initio, and SWS data at higher temperatures. This situation is similar to our earlier observation[16] for neopentane. The calculated heats of formation for these systems are in reasonable agreement with NIST values and are generally within ±0.5 kcal/mol.

For esters, GA-predicted S^{298K} values differ very significantly (3−4 cal/mol K) from the ab initio-computed values. As discussed in section A, although there are many stable conformers (viz., (sp, ap), (sp, sc), (sp, ap), (ap, sp), (ap, sc), (ap, ap)) with respect to the two dihedral angles about the C(O)−O and O−C bonds of the ester functionality, the differences seem to be too large to be accounted for by conformational contributions. Because experimentally determined entropy values are not available for two of the three esters studied here, namely, methyl propanoate and ethyl formate, we performed additional calculations on methyl formate and methyl acetate to identify the origin of the mismatch and to establish the extent of reliability of the ab initio values.

Recently, Van der Veken and co-workers[39] analyzed ethyl formate in the gas phase by electron diffraction and microwave and vibrational spectroscopy. Therefore, we calculated the entropy of this system using experimental vibrational frequencies and moments of inertia. The authors have characterized 25 of 27 vibrational frequencies and have analyzed the normal modes and their absorptions. The two unidentified vibrations correspond to the torsion around the O−C bond of the alcohol part of the ester and the COC bending (C(O)−O−C) vibration. The other two torsional vibrations, namely, around the C−C and CO−O bonds, were found at 228 and 311 cm^{-1}, respectively. The HF/6-31G(d′) calculated frequencies corresponding to these low-frequency torsional vibrations agree well after appropriate scaling (232 and 320 cm^{-1}). Consequently, while calculating the entropy for the COC bending vibration, we used our ab initio numbers, and we treated the three torsional modes as hindered rotations defined by the ab initio hindrance potentials. The result is very close to the one obtained solely from ab initio data and confirms the accuracy of the calculations. The results are shown in Table 5.

Our findings indicate that the probable error in the literature entropy group value for the {O/CO/C} group is 3−4 cal/mol K. Additionally, we also evaluated the Therm software[40] and the new groups developed by Bozzelli. The two groups associated with the ester functionality are {CO/O/C} and {O/CO/C}. The former group is present in the acids as well. To our surprise, Therm uses an entropy value of 10.04 cal/mol K for the {CO/O/C} group compared to Benson's value of 14.8 cal/mol K. The Therm value for {O/CO/C} group is the same

TABLE 6: Comparison of Calculated Thermodynamic Properties of C_2H_5X with Literature Values

species	method	$\Delta_f H_{298}$ (kcal/mol)	S^{298} (cal/mol K)	C_p^{300} (cal/mol K)	C_p^{400} (cal/mol K)	C_p^{500} (cal/mol K)	C_p^{600} (cal/mol K)	C_p^{800} (cal/mol K)	C_p^{1000} (cal/mol K)	C_p^{1500} (cal/mol K)
$CH_3CH_2CH{=}CH_2$	ab initio	0.45	73.00	20.69	25.95	30.77	34.93	41.60	46.64	54.55
	SWS	−0.03	73.04	20.57	26.04	30.93	35.14	41.80	46.82	
	GA(Benson)	0.09	73.50	20.61	26.17	31.08	35.28	41.98	46.98	54.78
	therm	−0.11	73.61	20.57	26.09	31.04	35.28	41.96	46.97	54.75
	NIST	−0.15	73.10	20.55	25.93	30.85	35.07	41.80	46.85	54.71
CH_3CH_2CCH	ab initio	39.07	68.66	19.14	23.66	27.52	30.77	35.92	39.82	45.96
	SWS	39.48	69.51	19.54	23.87	27.63	30.83	35.92	39.84	
	GA(Benson)	39.75	69.47	19.58	23.95	27.67	30.83	35.97	39.85	46.99
	therm	39.55	69.58	19.55	23.87	27.63	30.83	35.95	39.84	46.98
	NIST	39.48	69.60	19.64	24.06	27.87	31.08	36.19	40.05	46.13
CH_3CH_2Cl	ab initio	−26.19	65.78	14.86	18.25	21.34	23.96	28.09	31.18	35.99
	SWS	−26.70	65.93	15.05	18.56	21.68	24.31	28.42	31.48	
	GA(Benson)	−26.50	65.92	15.13	18.62	21.74	24.19	28.34	31.48	
	therm	−26.80	66.29	14.97	18.46	21.52	24.10	28.19	31.25	36.07
	NIST	−26.84								
$CH_3CH_2CH_2Cl$	ab initio	−31.87	74.79	20.28	25.15	29.57	33.32	39.22	43.58	50.33
	SWS	−31.10	76.27	20.34	25.36	29.73	33.43	39.24	43.59	
	GA(Benson)	−31.50	75.32	20.63	25.59	29.98	33.53	39.42	43.82	
	therm	−31.93	75.82	20.43	25.33	29.73	33.45	39.24	43.58	50.24
	NIST	−31.67								
CH_3CHCl_2	ab initio	−32.08	72.51	18.05	21.60	24.64	27.11	30.79	33.41	37.35
	SWS	−31.05	72.89	18.29	21.85	24.82	27.24	30.85	33.45	
	GA(Benson)	−28.90	71.82	18.33	21.92	24.84	27.29	30.94	33.48	
	therm	−31.24	73.14	18.18	21.82	24.93	27.41	31.11	33.57	37.01
	NIST	−30.50								
CH_3CCl_3	ab initio	−36.36	76.20	21.90	25.43	28.26	30.49	33.69	35.83	38.86
	GA(Benson)	−30.70	76.33	22.53	25.92	28.54	30.59	33.64	35.78	
	therm	−34.04	76.73	22.02	25.70	28.65	30.89	34.08	35.98	39.00
	NIST	−34.51								
CH_3CH_2F	ab initio	−65.24	63.11	14.03	17.35	20.47	23.19	27.53	30.77	35.80
	SWS	−62.50	63.32	14.17	17.57	20.72	23.44	27.76	30.98	
	GA(Benson)	−61.50	63.52	14.33	17.92	21.44	23.79	28.24	31.38	
	therm	−62.90	63.12	14.27	17.77	20.96	23.69	28.08	31.28	
$CH_3CH_2CH_2F$	ab initio	−70.08	72.41	19.27	24.13	28.63	32.50	38.60	43.12	50.08
	SWS	−67.20	72.71	19.83	24.55	28.99	32.82	38.88	43.37	
	GA(Benson)	−66.50	72.92	19.83	24.89	29.68	33.13	39.32	43.72	
	therm	−67.90	72.52	19.77	24.74	29.20	33.03	39.16	43.62	
$CH_3CH_2NH_2$	ab initio	−12.08	67.30	16.86	20.96	24.75	28.04	33.36	37.44	44.02
	SWS	−11.00	68.19	17.44	21.65	25.44	28.68	33.89	37.88	
	GA(Benson)	−11.80	67.62	17.20	21.33	25.04	28.25	33.54	37.59	
	therm	−11.80	67.63	17.20	21.33	25.04	28.25	33.54	37.59	44.17
CH_3CH_2SH	ab initio	−11.33	70.71	17.34	20.83	24.00	26.76	31.24	34.67	40.10
	SWS	−11.02	70.77	17.44	21.08	24.36	27.21	31.83	35.38	
	GA(Benson)	−11.03	70.73	17.47	21.20	24.55	27.54	32.60	36.64	
C_2H_5OH	ab initio	−55.97	66.81	15.75	19.21	22.52	25.43	30.12	33.70	39.39
	SWS	−56.12	67.54	15.71	19.36	22.77	25.69	30.33	33.83	
	GA(Benson)	−56.00	66.99	15.52	19.17	22.54	25.42	30.15	33.71	
	therm	−56.20	67.10	15.48	19.19	22.52	25.45	30.15	33.71	
	NIST	−56.23	67.50	15.65	19.41	22.89	25.87	30.57	34.10	39.68

as that given in Benson's table. As a result, the entropy predictions using Therm values appear to be incorrect for acids[17] whereas for esters other than formates they work very well. To obtain good predictions of S^{298} for both acids and esters, we believe that Benson's group value of {O/CO/C} needs to be revised, not the {CO/O/C} group value.

Benson's original group additivity values are known to perform poorly for chlorofluorocarbons as compared to that for hydrocarbons and oxygenated hydrocarbons. Yamada and Bozzelli[41] have developed new groups and interaction terms for the estimation of the thermochemical properties of hydrochlorofluoro- carbons. In Table 6, we present the estimates from both of the group values. Within this work, we are concerned about only {C/C/F/H2}, {C/C/Cl/H2}, {C/C/Cl2/H}, and {C/C/Cl3/H}. It is evident that Bozzelli's new groups provide a better prediction for the heat of formation values. In Table 6, the CBS-Q method seems to overestimate the stability of fluorocarbons by nearly 3 kcal/mol compared to the GA values. However, this mismatch cannot be considered seriously when one is evaluating the performance of the CBS-Q method. Recently, Benson[42] has reexamined the heat of formation data of all alkyl fluorides and has recommended a value of −66.6 ± 1 kcal/mol for ethyl fluoride, which is in excellent agreement with the CBS-Q predictions. The CBS-Q S and $C_p(T)$ values are in good agreement (within a few tenths cal/(mol K)) with GA values.

Because we are not deriving supergroups for the abstraction of hydrogen from the carbon containing fluorine, $-CH_xF_y$, discrepancies between ab initio data and GA values for halogen-containing groups, if any, are not expected to introduce significant error into the {C/C/H2/−H/Y} supergroups. Because the CH_2X group is common in both the reactant and transition structures, one can anticipate that the errors introduced into the method by X are effectively canceled out.

E. Comparison of Supergroup Thermodynamic Values. In Tables 7 and 8, we present the thermodynamic values of the reactive moiety for the individual abstraction reactions by H and CH_3, respectively. A quick glance at Tables 7 and 8 reveals that the ΔH^{298}, S^{298}, and $C_p(T)$ values at lower temperatures do not remain constant for all X. As anticipated from our discussion in section B, the ΔH^{298} value of the supergroup varies throughout the series. The range of the ΔH^{298} value is larger

TABLE 7: Group Additivity Values for Transition-State Supergroup {C/C/H2/-H/H} Belonging to H Abstraction Reactions from CH_3CH_2X by H

reaction	$\Delta_f H_{298}$ (kcal/mol)	S^{298} (cal/mol K)	C_p^{300} (cal/mol K)	C_p^{400} (cal/mol K)	C_p^{500} (cal/mol K)	C_p^{600} (cal/mol K)	C_p^{800} (cal/mol K)	C_p^{1000} (cal/mol K)	C_p^{1500} (cal/mol K)	ν_{imag} (cm^{-1})
$HCH_2CH_3 + H$	50.81	35.21	9.37	11.78	13.81	15.48	17.98	19.70	22.25	2227
$CH_3CH_2CH_3 + H$	50.94	34.94	9.49	11.90	13.91	15.56	18.02	19.72	22.25	2223
$(CH_3)_2CHCH_3 + H$	50.71	34.78	9.36	11.83	13.88	15.55	18.02	19.72	22.25	2225
$(CH_3)_3CCH_3 + H$	50.88	34.82	9.48	11.97	13.97	15.59	17.99	19.66	22.20	2204
$ClCH_2CH_3 + H$	52.05	34.17	10.61	12.65	14.40	15.88	18.18	19.82	22.30	2289
$HSCH_2CH_3 + H$	50.74	34.00	10.59	12.70	14.50	16.00	18.30	19.91	22.35	2264
$NH_2CH_2CH_3 + H$	51.23	34.35	11.18	13.05	14.70	16.11	18.33	19.91	22.34	2206
$HOCH_2CH_3 + H$	51.47	35.08	10.39	12.45	14.26	15.80	18.16	19.81	22.31	2211
$OHCCH_2CH_3 + H$	51.61	34.88	9.02	11.53	13.70	15.48	18.09	19.85	22.39	2235
$CH_3COCH_2CH_3 + H$	51.38	35.27	9.06	11.37	13.48	15.25	17.91	19.71	22.33	2224
$HOOCCH_2CH_3 + H$	51.65	35.09	8.80	11.38	13.60	15.39	18.03	19.81	22.38	2241
$CH_3OC(O)CH_2CH_3 + H$	51.47	35.15	8.81	11.38	13.57	15.37	18.00	19.77	22.35	2234
$CH_3OCH_2CH_3 + H$	51.85	35.29	9.48	11.80	13.81	15.48	18.00	19.73	22.28	2245
$HC(O)OCH_2CH_3 + H$	52.24	35.00	9.84	12.11	14.02	15.60	18.04	19.79	22.44	2264
$CH_3C(O)OCH_2CH_3 + H$	52.05	35.22	9.91	12.19	14.11	15.69	18.08	19.77	22.37	2258
$CH_2{=}CHCH_2CH_3 + H$	51.15	34.66	9.81	12.18	14.15	15.76	18.17	19.83	22.32	2227
$Cl_2CHCH_3 + H$	52.21	34.01	9.82	12.22	14.18	15.76	18.14	19.80	22.30	2316
$HCCCH_2CH_3 + H$	51.84	35.09	9.60	11.90	13.88	15.52	18.00	19.72	22.27	2233
$Cl_3CCH_3 + H$	52.72	34.71	9.51	12.04	14.10	15.75	18.17	19.83	22.30	2333
$FCH_2CH_3 + H$	52.42	35.11	9.47	11.86	13.87	15.52	18.00	19.72	22.27	2266
$ClCH_2CH_2CH_3 + H$	51.10	35.09	9.35	11.78	13.83	15.51	18.01	19.73	22.27	2269
$FCH_2CH_2CH_3 + H$	51.37	34.91	9.45	11.84	13.87	15.53	18.02	19.73	22.27	2265
{C/C/H2/-H/H}ave	51.60	34.86	9.65	11.99	13.98	15.62	18.07	19.78	22.31	2248
std deviation	0.59	0.39	0.60	0.43	0.30	0.21	0.11	0.07	0.06	33.5

TABLE 8: Group Additivity Values for Transition-State Supergroup {C/C/H2/-H/C/H3} for the H Abstraction Reaction from CH_3CH_2X by the CH_3 Radical

reaction	$\Delta_f H_{298}$ (kcal/mol)	S^{298} (cal/mol K)	C_p^{300} (cal/mol K)	C_p^{400} (cal/mol K)	C_p^{500} (cal/mol K)	C_p^{600} (cal/mol K)	C_p^{800} (cal/mol K)	C_p^{1000} (cal/mol K)	C_p^{1500} (cal/mol K)	ν_{imag} (cm^{-1})
$HCH_2CH_3 + CH_3$	37.83	49.40	14.41	17.85	20.84	23.41	27.52	30.60	35.52	2544
$CH_3CH_2CH_3 + CH_3$	37.77	48.76	14.52	17.93	20.90	23.45	27.54	30.62	35.53	2544
$(CH_3)_2CHCH_3 + CH_3$	37.68	48.73	14.69	18.11	21.06	23.57	27.60	30.64	35.52	2547
$(CH_3)_3CCH_3 + CH_3$	37.37	48.05	14.63	18.14	21.13	23.66	27.69	30.71	35.56	2555
$ClCH_2CH_3 + CH_3$	37.40	47.71	15.52	18.64	21.40	23.80	27.71	30.70	35.54	2542
$HSCH_2CH_3 + CH_3$	37.17	47.62	15.68	18.76	21.50	23.90	27.80	30.78	35.60	2544
$H_2NCH_2CH_3 + CH_3$	37.94	49.45	14.97	18.26	21.13	23.61	27.61	30.65	35.53	2537
$HOCH_2CH_3 + CH_3$	38.12	49.86	15.05	18.36	21.24	23.70	27.68	30.69	35.55	2532
$OHCCH_2CH_3 + CH_3$	37.59	49.42	14.47	17.97	21.02	23.62	27.74	30.80	35.66	2551
$CH_3COCH_2CH_3 + CH_3$	37.37	50.00	14.60	18.10	21.10	23.65	27.73	30.78	35.64	2551
$HOOCCH_2CH_3 + CH_3$	37.63	49.57	14.91	18.29	21.24	23.77	27.82	30.85	35.67	2555
$CH_3OC(O)CH_2CH_3 + CH_3$	37.61	50.04	14.96	18.30	21.23	23.75	27.78	30.82	35.66	2554
$CH_2{=}CHCH_2CH_3 + CH_3$	37.69	47.99	14.92	18.32	21.23	23.73	27.73	30.75	35.59	2543
$CH_3OCH_2CH_3 + CH_3$	38.08	50.06	14.77	18.23	21.18	23.69	27.70	30.73	35.59	2549
$HC(O)OCH_2CH_3 + CH_3$	38.14	50.09	14.89	18.22	21.11	23.61	27.64	30.69	35.59	2550
$CH_3C(O)OCH_2CH_3 + CH_3$	38.40	49.95	14.54	18.00	20.96	23.48	27.52	30.57	35.46	2550
{C/C/H2/-H/C/H3}	37.74	49.38	14.84	18.22	21.14	23.65	27.68	30.71	35.57	2546
std deviation	0.33	0.73	0.35	0.24	0.17	0.13	0.10	0.08	0.06	6.5

for {C/C/H2/−H/H} than for {C/C/H2/−H/C/H3} whereas the ordering for the S^{298} range is the reverse. The latter is probably due to the low-frequency wagging modes of the CH_2- - - H- - - CH_3 vibrations. However, it must be realized that we have examined more reactions in the case of H abstraction by H atom compared to the number of H abstractions by CH_3. Though the standard deviation for the average ΔH^{298} value of the {C/C/H2/−H/H} supergroup is only 0.59 kcal/mol, the overall variation is more than 2 kcal/mol. Consequently, the per hydrogen abstraction rate from the β carbon varies up to a factor of 29 at room temperature as the substituent is varied.

In Table 9, we present the TST rate constant, $k(T)$, for unsubstituted ethane at selected temperatures and compare this rate with the rates for substituted ethanes by providing the ratio of the rate constants, $k(CH_3CH_3 + H)/k(CH_3CH_2X + H)$. The TST rate constants were computed using the ab initio geometrical and molecular parameters and were corrected for tunneling using the simple Wigner correction.[43] It is evident that at high temperatures (e.g., at $T = 1500$ K) the rate constants for all monosubstituted ethanes with H agree within a factor of 2, which reflects the fact that substitution mainly affects the enthalpy but has little effect on the entropy of the supergroup. However, the discrepancy factor (e.g., 29) in the calculated rate at low T is quite large, and it requires us to allow the enthalpy of the supergroup to depend on non-next-neighbor substituents. It must be stated that there are no experimental data on the rate constant of β-hydrogen abstraction from substituted ethanes. For propane, *tert*-butane, and neopentane, experiments were done to estimate only the total hydrogen abstraction rate coefficient. For the latter two systems, the only reliable measurement is from Baldwin and Walker[44] at 753 K. Experiments on chloroethane[45] and ethanol[46] illustrate the occurrence of secondary

TABLE 9: Wigner Tunneling-Corrected Transition-State Theory Rates Per Hydrogen for Abstraction from Ethane by H Atom and the Ratio of Per Hydrogen Abstraction Rates for Substituted Ethanes, ($k(CH_3CH_3 + H)/k(C_2H_5X + H)$)

substituent, X	300 K	900 K	1500 K
CH_3CH_3	4.85×10^{6} [a]	1.60×10^{11} [a]	2.25×10^{12} [a]
CH_2Cl	12.86	2.80	1.99
CH_2OH	7.25	2.16	1.57
CH_2NH_2	3.52	1.80	1.48
CH_2SH	1.61	1.47	1.37
CH_2CHO	7.84	2.31	1.79
CH_2COCH_3	4.20	1.70	1.44
CH_2COOH	8.02	2.23	1.73
CH_2COOCH_3	5.81	1.97	1.59
CH_2OCH_3	5.47	1.70	1.35
CH_2OCOH	11.94	2.30	1.63
CH_2OCOCH_3	7.74	1.82	1.34
CH_2CHCH_2	2.34	1.48	1.31
CH_2CCH	6.28	1.98	1.56
$CHCl_2$	18.14	3.60	2.55
CCl_3	29.32	3.44	2.20
CH_2F	15.28	2.52	1.75
CH_2CH_2F	1.69	1.24	1.16
CH_2CH_2Cl	2.92	1.56	1.37

[a] cm^3/mol s.

TABLE 10: Calculated Inductive (σ^*), Steric (R_s), and Hyperconjugative (*HC1*) Effects of the CH_3- --L Substituents Using Atomic Additivity Rules[a]

substituent (L)	(σ^*)	R_s	χ_g	*HC1*	alkyl substituent	R_s
CH_2OH	0.55	−1.477	2.518	−4.45	CH_3CH_3	−1.182
CH_2OCH_3	0.58	−1.686	2.527	−4.45	$CH_3CH_2CH_3$	−1.583
$CH_2OC(O)H$	1.07	−1.741	2.544	−4.45	$CH_3(CH_2)_2CH_3$	−1.766
$CH_2OC(O)CH_3$	1.08	−1.876	2.546	−4.45	$(CH_3)_3CH$	−2.000
$CH_2C(O)H$	1.05	−1.699	2.479	−5.30	$CH_3(CH_2)_3CH_3$	−1.881
$CH_2C(O)CH_3$	1.08	−1.891	2.483	−5.30	$(CH_3)_2CHCH_2CH_3$	−2.202
$CH_2C(O)OH$	1.28	−1.832	2.496	−5.30	$(CH_3)_2CHCH_2CH_3$	−2.067
$CH_2C(O)OCH_3$	1.29	−1.958	2.497	−5.30	$(CH_3)_4C$	−2.455
CH_2Cl	1.03	−1.570	2.537	−5.30	$CH_3CH_2CH_3$	−2.479
CH_2NH_2	0.30	−1.543	2.472	−5.30	$CH_3CH_2CH_2CH_3$	−2.919
CH_2SH	0.65	−1.651	2.436	−6.30	$CH_3CH_2CH_2CH_2CH_3$	−3.121
$CH_2CH{=}CH_2$	0.16	−1.693	2.439	−5.30	$(CH_3CH_2)_2CH_2$	−3.373
CH_2CCH	0.70	−1.611	2.448	−4.45	$(CH_3)_2CHCH_2CH_3$	−3.372
$CHCl_2$	2.08	−1.972	2.674	−5.30	$(CH_3)_3CH$	−3.913
CCl_3	3.16	−2.387	2.811	−5.30	$(CH_3)_2CHCH_2CH_3$	−4.379
CH_2F	1.05	−1.415	2.654	−3.80		
CH_2CH_2Cl	0.45	−1.763	2.448	−5.30		
CH_2CH_2F	0.42	−1.678	2.465	−5.30		

[a] Group electronegativities are calculated using Pauling's electronegativity scale and "super atom" approach.

hydrogen abstraction whereas in thioethanol[47] the hydrogen from SH is more labile than the C−H hydrogens. With unsaturated substituents, addition across the unsaturated bond is often the preferred pathway over abstraction at low *T*, and it competes with abstraction at high *T*. Consequently, we are not aware of many reliable experimental data to compare with our calculations.

Analysis of Table 7 reveals the following: (i) Among the investigated lone pair substituents, the magnitude of ΔH^{298} varies in the order $CH_2F > CH_2OC(O)H > CH_2Cl > CH_2OCH_3 > CH_2OH > CH_2NH_2 > CH_2SH$ and is parallel to the group electronegativity scale of the substituent (Table 10). The β-C−H bond strength follows the same trend except for chloroethane. (ii) The same observation holds as the number of same substituents increases. In the series CH_2Cl, $CHCl_2$, and CCl_3, the enthalpy value of the supergroup as well as the β-C−H bond strength increases with increasing group electronegativity. However, the increment in ΔH^{298K} per chlorine atom is not the same as one goes from mono to di or from di to tri substitution. This is probably due to the unfavorable valence-angle strain in di- and trisubstituted reactants, which contribute to the reaction barrier. (iii) Within the series of investigated π-acceptor substituents, the enthalpy of the {C/C/H2/−H/H} supergroup follows the same order as the group electronegativity (viz., $CH{=}CH_2 < CCH < CHO < COOH$). (iv) Though the group electronegativity remains nearly the same for the pairs (a) OC(O)H and $OC(O)CH_3$, (b) CHO and $COCH_3$, and (c) COOH and $COOCH_3$, the enthalpy of the supergroup decreases by ∼0.2 kcal/mol in each pair with methyl substitution, which suggests that the barrier height correlates with both the electronic and size factors of the substituent. (v) Cl and F substituents γ to the bond being attacked do not exert a significant effect on the {C/C/H2/−H/H} supergroup, essentially because the magnitude of the through-bond interaction decreases drastically as the number of intervening bonds increases. Also, if the substituent is farther away from the reaction center, the bulkiness of the substituent does not have much effect on the screening of the reaction center. (vi) Analysis of S^{298} values of the supergroup among the monosubstituted systems reveals that the entropy is lower for the third-row substituents Cl and SH.

Comparison of the results in Tables 7 and 8 reveals the following: (i) O-centered substituents (OH, OCH_3, OC(O)H, and $OC(O)CH_3$) increase the barrier height for abstraction compared to that of ethane. The increase is larger for abstraction by H than by CH_3. (ii) SH lowers the barrier height to a greater extent for CH_3 than for H. (iii) π-acceptor substituents (viz., CHO, $COCH_3$, COOH, and $COOCH_3$) increase the barrier height by nearly 0.7 kcal/mol for the reaction with H but have no significant effect on the barrier with CH_3. (iv) Similarly, the Cl atom has the opposite effect on barrier heights with H and CH_3. (v) Both Cl and SH substituents exert the same effect of lowering the entropy of {C/C/H2/−H/H} and {C/C/H2/−H/C/H3} supergroups. Both H and CH_3 are nonpolar radicals differing in their size and structure. Consequently, the relative differences in ΔH^{298} of {C/C/H2/−H/H} and {C/C/H2/−H/C/H3} supergroups suggest that nature of the attacking radical plays a role in estimating the barrier height in addition to the electronic and steric nature of the substituent.

F. Rudimentary Procedure to Accommodate Non-Next Neighbor Effects. Our goal is to build meaningful and thermodynamically consistent rate estimates for different types of reactions using high-level quantum chemical calculations and to validate their performance simultaneously by comparison with experimental rate coefficients. The challenge is to rationalize all the observations mentioned above on the individual systems and then to develop efficient general methods to account for non-next-neighbor effects. Because the S^{298} and $C_p(T)$ values for the supergroups do not depend strongly on non-next-neighbor substituents, we start by using the same *S* and $C_p(T)$ values for all members of a reaction family. The supergroups' ΔH^{298} values are more sensitive to the substituent X, so below we propose ways of accounting for this variation without requiring a new quantum chemical calculation each time the substituent is varied.

The calculated σ^* and steric parameters of the substituents L (in most cases, $L = CH_2X$) are shown in Table 10 along with the group electronegativity values χ_g. While calculating σ^* and R_s, the carbon atom of the reactive moiety, CH_2- - - H- - - Y, is taken as the reaction center. In both of the series, the inductive and steric effects of the substituent remain exactly the same. However, with CH_3 as the abstracting radical, one expects additional steric interactions that are not captured by Galkin and Cherkasov's R_s parameter. The calculated R_s value is just a measure of the mechanical screening of a reaction

center by L, and it does not account for valence-angle strain for interactions between Y and L.

The conventional procedure, by analogy to what is usually done with experimental rates, would be to plot $\log(k(XCH_2\text{-}CH_3 + H)/k(CH_3CH_3 + H))$ versus σ^* or R_s and look for linear correlation, assuming that the rest of the interactions, if any, remain the same between substituted and unsubstituted systems. Such a procedure would work well for monosubstituted systems of similar substituent characteristics. However, it would be much more convenient to have a single expression that worked for multiple and a broad range of substituents X, so we took a more general approach. The CBS-Q barrier heights for abstraction of the primary hydrogen from alkanes by H were initially fitted to a multilinear expression

$$\text{Barrier (kcal/mol)} = a_0 + a_1\sigma^* + a_2R_s$$

which results in an a_0 value of 9.757 kcal/mol. Because the value of σ^* is zero for alkyl substituents and H and $R_s(H) = 0.0$, the intercept should correspond to the barrier height for the abstraction from CH_4, which at the same level of theory has been calculated[16] to be 12.989 kcal/mol. A combined fit including the barrier heights for 1°, 2°, and 3° abstractions yielded a more reasonable value of 12.867 kcal/mol for a_0, but the fit exhibited significant deviations suggesting the involvement of some other substituent effect in addition to inductive and steric effects. Similarly, unsatisfactory fits were obtained when fitting the bond dissociation energies of alkanes using only these two parameters (σ^* and R_s). This result led us to search for a third physical phenomenon that could explain the non-next-neighbor effects on C−H BDE values and abstraction barrier heights. We identified the hyperconjugative effect (e.g., $CH_3CH_2^{\bullet} \leftrightarrow H^{\bullet}CH_2{=}CH_2$) as the additional cause for the increasing stability of the product radicals or the decreasing bond strength as one goes from methane to primary to secondary to tertiary C−H bonds. In transition structures, this effect involves the interaction between the C−H bond orbital being broken and the C−H and C−X bonds on the β carbon. By the Hammond postulate, this effect that is thought to dominate in alkyl radical stability should also influence the barrier to formation of the radicals. When one considers only the effects of an alkyl substituent on a single reaction family, the contribution from hyperconjugative interaction is nearly the same, and this effect is largely canceled out by the ratio used in the conventional Taft procedure described above.

Because we do not have a method for quantitatively estimating the hyperconjugative effect, we derived these parameters by following the systematic deviations observed in the BDE fit to σ^* and R_s. As one goes from 1° to 2° to 3° radicals or abstraction transition structures, the number of β C−H bonds overlapping with the radical center increases. Because of symmetry, all β C−H bonds in the same plane as the radical center overlap effectively with the radical center and thereby contribute to the stabilization of the radical. However, the alkyl groups adjacent to the radical center ($R\text{-}\text{-}CH_2$) can rotate freely, thus enabling the overlap of other β-C−H bonds with the radical center. Hence, in the present work, we are concerned with an effective hyperconjugative interaction parameter for the β group. Good fits were obtained for the BDE using the expression

$$\text{BDE (kcal/mol)} = a_0 + a_1\sigma^* + a_2R_s + a_3^*HC1 + a_4^*HC2 + a_5^*HC3$$

with $HC1 = -5.30$, $HC2 = -4.10$, and $HC3 = -2.90$ kcal/mol for the hyperconjugative interaction with the first, second, and third CH_2R groups as one goes from $RCH_2C\mathbf{H}_3\bullet$ to $(RCH_2)_2C\mathbf{H}_2$ to $(RCH_2)_3C\mathbf{H}$ systems. The coefficients a_3, a_4 and a_5 are chosen to be nearly unity such that *HC1* is a measure of the hyperconjugative interaction with an $L = CH_2R$ group. In the case of secondary and tertiary hydrogen abstractions, the reactants $(RCH_2)_2CH_2$ and $(RCH_2)_3CH$ experience valence-angle strain because of bulky multiple substituents at the same carbon. This strain decreases at the transition structure and vanishes in the product radical, and this strain release is thus expected to contribute to the barrier height and BDE values of secondary and tertiary C−H bonds. Consequently, the magnitude of *HC2* and *HC3* terms are smaller than that of *HC1* terms. In other words, the *HC2* and *HC3* parameters are a measure of combined effects because the estimated steric effect, R_s, of X does not account for the valence-angle strain.

For all substituents where the proximate atom in X is carbon (e.g., CHO, $COCH_3$, COOH, $COOCH_3$, $CH{=}CH_2$, CCH), we assumed the hyperconjugative interaction (*HC1*) to be the same (−5.30) as that for primary alkyl substituents. Because oxygen and fluorine are more electronegative than carbon, we assumed a slightly smaller stabilization (−4.45) for all O-centered substituents (OH, OCH_3, OC(O)H, $OC(O)CH_3$) and F (−3.80) compared to that of C-centered substituents (Table 10). The CBS-Q energy differences between the gauche and anti conformers (with respect to the $XCH_2\text{-}\text{-}\text{-}CH_2$(HH) bond) of the transition-state structures (see Table 2) are ∼0.6 and ∼0.3 kcal/mol, respectively, for all O-centered and C-centered X groups. This energy difference is roughly a measure of the difference in the hyperconjugating efficiency of β-C−H and β-C−X bonds. To be consistent with the *HC1* parameters for other groups used in fitting the quantum calculations, we assigned values of −5.30 to chlorine and −6.30 to the SH group (Table 10). Subsequently, we derived the best-fit expressions for the BDE and barrier heights for H abstraction by H and CH_3 in alkanes and substituted alkanes (Figure 6):

$$\text{BDE (kcal/mol)} = 103.692 + 0.379\sigma^* - 1.149\,R_s + 1.004HC1 + 0.999HC2 + 1.017HC3$$

$$\text{Barrier(H) (kcal/mol)} = 12.966 + 0.681\sigma^* + 0.253R_s + 0.531HC1 + 0.645HC2 + 0.572HC3$$

$$\text{Barrier}(CH_3)\text{ (kcal/mol)} = 17.060 + 0.036\sigma^* + 0.542R_s + 0.474HC1 + 0.488HC2 + 0.291HC3$$

The intercept for the methyl abstraction barrier is in good agreement with the CBS-Q barrier height for the reaction $CH_4 + CH_3 \rightarrow CH_4 + CH_3$ (16.980 kcal/mol).[16] The coefficients of the multilinear expression for the barrier height to reaction with CH_3 vary from that for reactions with H. Because the former includes the steric interactions between Y and X, this is particularly significant for abstraction from tertiary C−H groups because of steric crowding. The correlation of the fitted barrier heights and BDE values are shown in Figure 6. The sum of the squared deviations (differences between the actual value of the barrier height for each reaction and the value predicted by the fitted function) for the fitted barrier heights with H and CH_3 are, respectively, 1.85 and 1.61 kcal/mol.

It is interesting to note that the fitted coefficients of the *HC* terms in the multilinear expression for the barrier heights are about half as big as those for the BDEs. We believe this is because the reactions considered in this work are nearly thermoneutral, so the TS is about halfway to the radical product. As discussed earlier, hyperconjugative interactions appear to

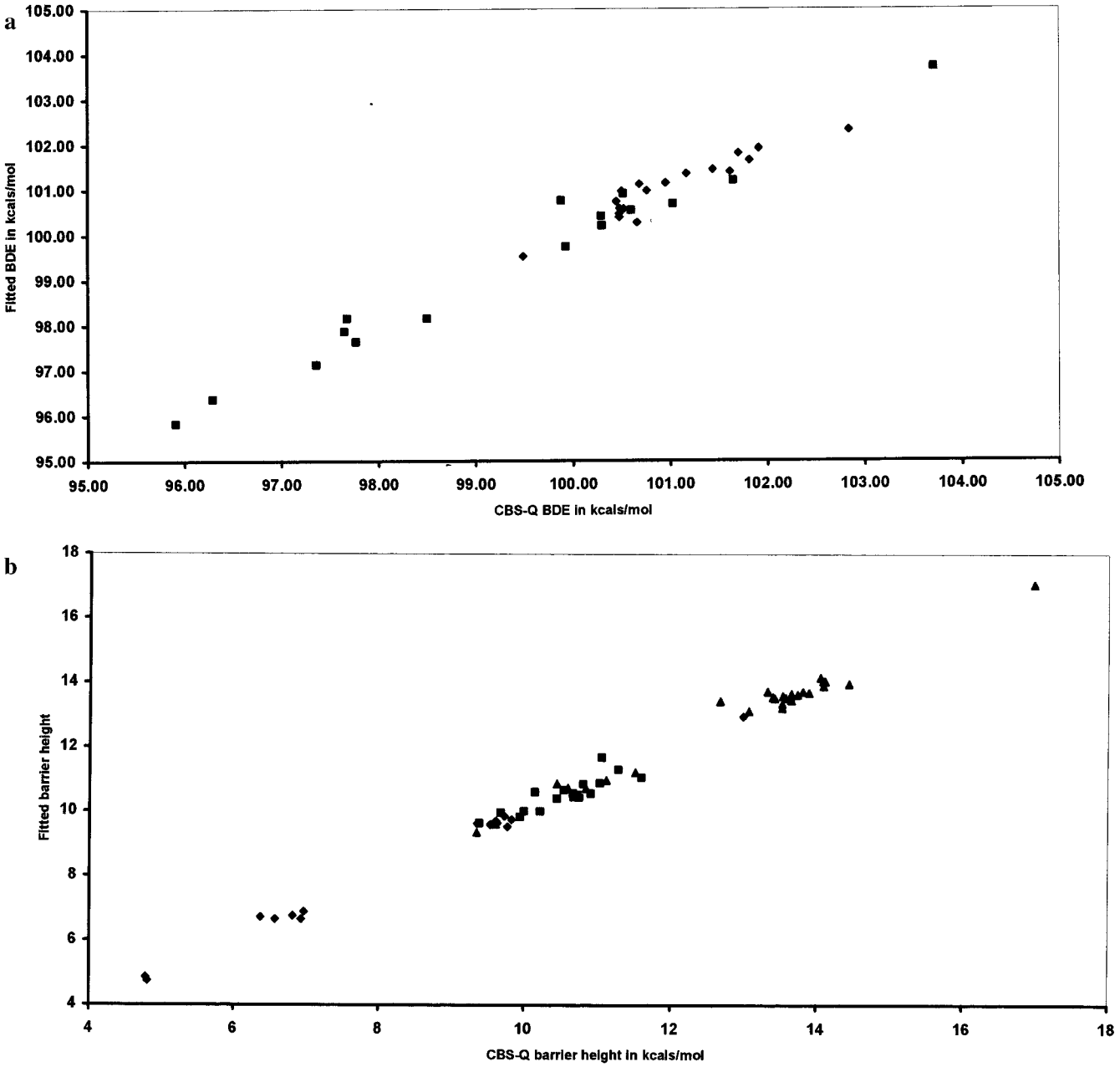

Figure 6. (a) Correlation of the CBS-Q computed bond dissociation energies with the fitted bond dissociation energies in kcal/mol. The filled squares correspond to the BDE of the C−H bond in alkanes, and the filled diamonds correspond to those of substituted alkanes. (b) Correlation of the CBS-Q barrier heights with the fitted barrier heights in kcal/mol. The filled squares and triangles correspond, respectively, to abstraction from alkanes by H and a methyl group, and the filled diamonds correspond to abstraction from substituted alkanes.

dominate in abstraction barrier heights, though some other smaller physical effects are also lumped into the *HC2* and *HC3* parameters as derived from the fit.

In the present work, the substituents interact with the reaction center largely through hyperconjugative interactions because of the intervening CH_2 group. When the mediating group happens to be a carbonyl group (with π orbitals for interaction) or an atom with a lone pair of electrons, then an extended interaction of the substituent orbitals with the reaction center through delocalization is possible. In such cases, both the BDE and barrier height would then be functions of steric, inductive, and mesomeric parameters of the substituents. Work is in progress to understand the effect of substituents on hydrogen abstraction from carbonyl and oxy substrates. It is also of interest to investigate the H abstraction reactions by OH, owing to the richness of their available experimental data. Besides the vast literature on experimental data, several empirical structure activity relations have been developed for this family of reactions and are shown by Atkinson[48] to predict the reaction rates accurately. Consequently, application of our method to these reactions would provide a much more exacting test of the method. However, these reactions have very low or negative activation barriers and very floppy transition states requiring a variational transition-state theory treatment. Our current treatment based solely on E_a will not capture the entropic effects that are expected to be important in the OH systems.

Conclusions

A qualitative understanding of group additivity in transition structures has been derived through AIM analysis of hydrocarbons and transition structures involved in the primary hydrogen

abstraction reaction $CH_3R + H \rightarrow CH_2R + H_2$ (R = CH_3, C_2H_5, *n*-C_3H_7, *i*-C_3H_7, *n*-C_4H_9, *i*-C_4H_9, *sec*-C_4H_9, *t*-C_4H_9, *n*-C_5H_{11}, 2-C_5H_{11}, 3-C_5H_{11}, etc.). An analysis based on charge density surfaces suggests the operation of non-next-neighbor effects. In almost every case, the stabilization energy of the reactive moiety correlates roughly with the barrier height.

The effects of substituents on the bond strengths and reactivities of a β-C−H bond linked through a CH_2 group have been quantified at the CBS-Q level of treatment. By using substituted ethanes, CH_3CH_2X (X = H, CH_3, CH_2CH_3, $(CH_3)_2$-CH, $C(CH_3)_3$, OH, OCH_3, OC(O)H, $OC(O)CH_3$, CHO,$COCH_3$, COOH, $COOCH_3$, Cl, SH, NH_2, F, $CH{=}CH_2$, CCH), we have estimated the effects of alkyl, lone pair, and π-acceptor substitutions on bond strength and barrier height. We determined the dominating influence of the substituent to result from hyperconjugative interactions between the partially formed radical and the β-C−H or C−X bonds. The preferred conformation around the CH_2X- - - -CH_2(HY) bond in transition structures and product radicals is the net result of the effective overlap of the (forming) radical center and the β-C−H or β-C−X bond.

Our calculations further indicate the involvement of the inductive effect of the substituent in determining the bond strength and barrier height. This can be seen in the monotonic progression toward stronger C−H bonds and increased barrier heights with successive chloro substitution on the β carbon. As expected for an inductive effect, substitutents on the γ (e.g., propyl chloride and propyl fluoride) or δ carbon have much less influence on the C−H bond strength and barrier height. We therefore express the barrier heights and bond dissociation energies as a function of inductive, steric, and hyperconjugative effects of X. The former two interactions are estimated using well-known descriptors from the literature whereas we derive the hyperconjugative parameter from the best-fit expression for the BDE. Though we do not have a rigorous physical basis for quantifing the through-space hyperconjugative stabilization, our fitted expression for the barrier agrees well for all of the 60 systems investigated so far. *HC2* and *HC3* parameters are the net effect of both hyperconjugative and valence-angle strain, and the coefficients of the *HC* terms in the fitted barrier height with CH_3 account for steric interactions between Y and X as well.

We derive a multilinear expression for the barrier height that allows for substituent effects on the enthalpy of the supergroup while retaining most of the simplicity of the group additivity method for estimating reaction rates. In the same way, one can also arrive at multilinear expressions for entropy and heat capacity. Work is in progress to understand the effect of substituents with a mediator containing either a π (e.g., C=O) or n orbitals (e.g., O) and thus allowing for extended overlap between the substituent orbitals and the reaction center.

Acknowledgment. This work was partially supported by the National Computational Science Alliance under grants CTS010006N and utilized the Origin 2000 High-Performance Computing and UniTree Mass Storage systems. We are grateful for financial support from the EPA Center for Airborne Organics, the NSF CAREER program, Alstom Power, Dow Chemical and the Division of Chemical Sciences, the Office of Basic Energy Sciences, the Offices of Energy Research, and the U.S. Department of Energy through grant DE-FG02-98ER14914.

Supporting Information Available: The MP2/6-31G(d′) optimized geometries, unscaled harmonic frequencies in (cm^{-1}), and rotational constants (in GHz) of the reactants and transition structures are available as supplementary tables (S1−S3). This material is available free of charge via the Internet at http://pubs.acs.org.

References and Notes

(1) Green, W. H., Jr.; Barton, P. I.; Bhattacharjee, B.; Matheu, D. M.; Schwer, D. A.; Song, J.; Sumathi, R.; Carstensen, H.-H.; Dean, A. M.; Grenda, J. M. *Ind. Eng. Chem. Res.* **2001**, *40*, 5362.

(2) Susnow, R. G.; Dean, A. M.; Green, W. H., Jr.; Peczak, P.; Broadbelt, L. J. *J. Phys. Chem. A* **1997**, *101*, 3731.

(3) Klinke, D. J. I.; Broadbelt, L. J. *AIChE J.* **1997**, *43*, 1828. Klinke, D. J. I.; Broadbelt, L. J. *Chem. Eng. Sci*. **1999**, *54*, 3379.

(4) Sirdeshpande, A. R.; Ierapetritou, M. G.; Androulakis, I. P. *AIChE J.* **2001**, *47*, 2461.

(5) Song, J.; Stephanopoulos, G.; Green, W. H., Jr. *Chem. Eng. Sci.*, submitted for publication, 2001.

(6) Rabitz, H.; Kramer, M.; Dacol, D. *Annu. Rev. Phys. Chem*. **1983**, *34*, 419.

(7) Turanyi, T. *J. Math. Chem*. **1990**, *5*, 203.

(8) Benson, S. W. *Thermochemical Kinetics*; 2nd ed; Wiley-Interscience: New York, 1976.

(9) Cohen, N. *Int. J. Chem. Kinet.* **1982**, *14*, 1339. Cohen, N. *Int. J. Chem. Kinet.* **1983**, *15*, 503.

(10) Cohen, N.; Westberg, K. R. *Int. J. Chem. Kinet.* **1986**, *18*, 99.

(11) Atkinson, R.; Carter, W. P. L.; Aschmann, S. M.; Winer, A. M.; Pitts, J. N., Jr. *Int. J. Chem. Kinet.* **1984**, *16*, 469.

(12) Cohen, N.; Benson, S. W. *J. Phys. Chem.* **1987**, *91*, 171.

(13) Cohen, N. *Int. J. Chem. Kinet.* **1991**, *23*, 683. Cohen, N. *Int. J. Chem. Kinet.* **1991**, *23*, 397.

(14) Rodgers, A. S. *Int. J. Chem. Kinet.* **1993**, *25*, 41.

(15) Senosiain, J. P.; Musgrave, C. B.; Golden, D. M. *J. Phys. Chem. A* **2001**, *105*, 1669.

(16) Sumathi, R.; Carstensen, H.-H.; Green, W. H., Jr. *J. Phys. Chem.* **2001**, *105*, 6910.

(17) Sumathi, R.; Carstensen, H.-H.; Green, W. H., Jr. *J. Phys. Chem*. **2001**, *105*, 8969.

(18) Bader, R. F. W. *Atoms in Molecules: A Quantum Theory*; Oxford University Press: New York, 1990.

(19) Bader, R. F. W.; Bayles, D. *J. Phys. Chem. A* **2000**, *104*, 5579.

(20) Denisov, E. *General Aspects of the Chemistry of Radicals*; edited by Z. B. Alfassi, Ed.; John Wiley & Sons Ltd: Chichester, U.K., 1999; p 79.

(21) Galkin, V.; Cherkasov, R. *Org. React.* **1981**, *18*, 1 and references therein.

(22) Galkin, V. I.; Sayakhov, R. D.; Cherkasov, R. A. *Russ. Chem. Rev*. **1991**, *60*, 815.

(23) Cherkasov, A. R.; Galkin, V. I.; Cherkasov, R. A. *Russ. Chem. Rev.* **1996**, *65*, 641.

(24) Cherkasov, A. R.; Jonsson, M.; Galkin, V. I. *J. Mol. Graphics Modell.* **1999**, *17*, 28.

(25) Frisch, M. J.; Trucks, G. W.; Schlegel, H. B.; Scuseria, G. E.; Robb, M. A.; Cheeseman, J. R.; Zakrzewski, V. G.; Montgomery, J. A., Jr.; Stratmann, R. E.; Burant, J. C.; Dapprich, S.; Millam, J. M.; Daniels, A. D.; Kudin, K. N.; Strain, M. C.; Farkas, O.; Tomasi, J.; Barone, V.; Cossi, M.; Cammi, R.; Mennucci, B.; Pomelli, C.; Adamo, C.; Clifford, S.; Ochterski, J.; Petersson, G. A.; Ayala, P. Y.; Cui, Q.; Morokuma, K.; Malick, D. K.; Rabuck, A. D.; Raghavachari, K.; Foresman, J. B.; Cioslowski, J.; Ortiz, J. V.; Stefanov, B. B.; Liu, G.; Liashenko, A.; Piskorz, P.; Komaromi, I.; Gomperts, R.; Martin, R. L.; Fox, D. J.; Keith, T.; Al-Laham, M. A.; Peng, C. Y.; Nanayakkara, A.; Gonzalez, C.; Challacombe, M.; Gill, P. M. W.; Johnson, B. G.; Chen, W.; Wong, M. W.; Andres, J. L.; Head-Gordon, M.; Replogle, E. S.; Pople, J. A. *Gaussian 98*, revision A.9; Gaussian, Inc.: Pittsburgh, PA, 1998.

(26) Montgomery, J. A., Jr.; Ochterski, J. W.; Petersson, G. A. *J. Chem. Phys.* **1994**, *101*, 5900. Ochterski, J. W.; Petersson, G. A.; Montgomery, J. A., Jr. *J. Chem. Phys.* **1996**, *104*, 2598.

(27) Nicolaides, A.; Rauk, A.; Glukkhovtsev, M. N.; Radom, L. *J. Phys. Chem*. **1996**, *100*, 17460. Curtiss, L. A.; Raghavachari, K.; Redfern, P. C.; Pople, J. A. *J. Chem. Phys.* **1997**, *106*, 1063.

(28) Petersson, G. A.; Malick, D. K.; Wilson, W. G.; Ochterski, J. W.; Montgomery, J. A., Jr.; Frisch, M. J. *J. Chem. Phys*. **1998**, *109*, 10570 and references therein.

(29) Sumathi, R. *TSTHIR*, version 1.0.

(30) Biegler König, F. W.; Bader, R. F. W.; Tang, T. *J. Comput. Chem.* **1982**, *13*, 317. Biegler König, F. *J. Comput. Chem.* **2000**, *21*, 1040. *AIMPAC* software can be downloaded from http://www.chemistry.mcmaster.ca/aimpac/.

(31) (a) Eliel, E. L. *Stereochemistry of Organic Compounds*; Wiley & Sons: New York, 1994.

(32) Oyanagi, K.; Kuchitsu, K. *Bull. Chem. Soc. Jpn.* **1978**, *51*, 2237.

(33) McKean, D. C. *Chem. Soc. Rev.* **1978**, *7*, 399 and references therein. Nelson, R.; Pierce, L. *J. Mol. Spectrosc.* **1965**, *18*, 344. Swalen, J. D.; Costain, C. C. *J. Chem. Phys*. **1959**, *31*, 1562. Bowers, P.; Schafer, L. *J. Mol. Struct.* **1980**, *69*, 233.

(34) Guo, D.; Goodman, L. *J. Phys. Chem. A* **1996**, *100*, 12540.

(35) Henry, D. J.; Parkinson, C. J.; Mayer, P. M.; Radom, L. *J. Phys. Chem. A* **2001**, *105*, 6750.

(36) Smith, D. M.; Nicolaides, A.; Golding, B. T.; Radom, L. *J. Am. Chem. Soc.* **1998**, *120*, 10223.

(37) (a) NIST Webbook. http://webbook.nist.gov. (b) NIST Standard Reference Database 25, Structure and Properties, version 2.02.

(38) Stull, D. R.; Westrum, E. F., Jr.; Sinke, G. C. *The Chemical Thermodynamics of Organic Compounds*; Krieger Publishing: Malabar, FL, 1987.

(39) Peng, Z.; Shlykov, S.; Van Alsenoy, C.; Geise, H. J.; Van der Veken, B.; *J. Phys. Chem.* **1995**, *99*, 10201. Maes, I. I.; Herrebout, W. A.; Van der Veken, B. J. *J. Raman Spectrosc.* **1994**, *25*, 679.

(40) Ritter, E. R.; Bozzelli, J. W. *Int. J. Chem. Kinet.* **1991**, *23*, 767.

(41) Yamada, T.; Bozzelli, J. W. *J. Phys. Chem. A* **1999**, *103*, 7373.

(42) Luo, Y.-R.; Benson, S. W. *J. Phys. Chem. A* **1997**, *101*, 3042.

(43) Hirschfelder, J. O.; Wigner, E. *J. Chem. Phys*. **1939**, *7*, 616.

(44) Baldwin, R. R.; Walker, R. W. *J. Chem. Soc., Faraday Trans. 1* **1979**, *75*, 140.

(45) Manion, J. A.; Louw, R. *J. Chem. Soc., Perkin Trans. 2* **1988**, 1547.

(46) Mezyk, S. P.; Bartels, D. M. *J. Phys. Chem. A* **1997**, *101*, 1329. Ader, W. K.; Wagner, H. G. *Ber. Bunsen-Ges. Phys. Chem.* **1973**, *77*, 712. Bensol, K. M.; Freeman, G. R. *J. Am. Chem. Soc.* **1968**, *90*, 7183.

(47) Lam, W. W.; Yokota, T.; Safarik, I.; Strausz, O. P. *J. Photochem. Photobiol., A* **1989**, *47*, 48. Kuntz, K. *J. Phys. Chem.* **1967**, *71*, 3343.

(48) Atkinson, R. *Chem. Rev.* **1986**, *85*, 69.